

AI-AEC-12990
ENDF-150

AN EVALUATION
OF TANTALUM-181 AND TANTALUM-182
FOR THE ENDF/B DATA FILE

AEC Research and Development Report



Atomics International
North American Rockwell

P.O. Box 309
Canoga Park, California 91304

LEGAL NOTICE

This report was prepared as an account of work sponsored by the United States Government. Neither the United States nor the United States Atomic Energy Commission, nor any of their employees nor any of their contractors, subcontractors, or their employees, makes any warranty, express or implied, or assumes any legal liability or responsibility for the accuracy, completeness or usefulness of any information, apparatus, product or process disclosed, or represents that its use would not infringe privately owned rights.

Printed in the United States of America
Available from
National Technical Information Service
U.S. Department of Commerce
Springfield, Virginia 22151
Price: Printed Copy \$3.00; Microfiche \$0.65

AN EVALUATION
OF TANTALUM-181 AND TANTALUM-182
FOR THE ENDF/B DATA FILE

BY
E. H. OTTEWITTE
J. M. OTTER
P. F. ROSE
C. L. DUNFORD



Atomics International
North American Rockwell

P.O. Box 309
Canoga Park, California 91304

CONTRACT: AT(04-3)-824
ISSUED: SEPTEMBER 30, 1971

DISTRIBUTION

This report has been distributed according to the category "Physics" as given in the Standard Distribution for Unclassified Scientific and Technical Reports, TID-4500.

CONTENTS

| | Page |
|---|------|
| Abstract | 6 |
| I. Introduction | 7 |
| II. Evaluation of Cross Section Data Below 100 kev. | 8 |
| A. Resolved Resonance Region | 8 |
| 1. Evaluation Methods | 8 |
| 2. Positive Energy Resolved Resonance Parameters | 8 |
| 3. Upper Energy Limit of Resolved Resonance Range | 10 |
| 4. p-Wave Resolved Resonances | 10 |
| 5. Potential Scattering Cross Section | 11 |
| 6. Thermal Cross Sections and Negative Energy Resonances | 11 |
| 7. Tabulation of Resonance Parameters | 15 |
| B. Unresolved Resonance Region | 15 |
| 1. Methods of Evaluation | 15 |
| 2. Energy Range for Unresolved Resonances Region | 21 |
| 3. Average Parameters Derived From Resolved Resonances | 22 |
| 4. Experimental Data Evaluation for Unresolved Resonance Energy Range | 23 |
| 5. Parameter Fits to Experimental Data | 26 |
| 6. Comparison of Calculated and Measured Resonance Integrals | 27 |
| III. Evaluation of Cross Section Data Above 100 kev. | 34 |
| A. Theoretical Calculations | 34 |
| 1. Introduction | 34 |
| 2. Optical Model Calculations | 34 |
| 3. Statistical Compound Nucleus Calculation | 35 |
| B. Evaluated Data | 37 |
| 1. Radiative Capture Cross Sections | 37 |
| 2. Total Cross Section | 38 |
| 3. Elastic Cross Sections and Angular Distributions of Elastically Scattered Neutrons | 42 |
| 4. Inelastic Cross Section and Angular Distributions of Inelastically Scattered Neutrons | 45 |
| 5. Cross Sections for the (n,2n) and (n,3n) Reaction | 49 |

CONTENTS

| | Page |
|--|------|
| 6. Cross Sections for the (n, α) Reaction. | 51 |
| 7. Cross Sections for the (n,p) Reaction. | 51 |
| 8. Secondary Neutron Energy Distributions. | 51 |
| References | 55 |

TABLES

| | |
|---|----|
| 1. Resolved Resonance Parameters for Ta ¹⁸¹ | 17 |
| 2. Resolved Resonance Parameters for Ta ¹⁸² | 19 |
| 3. Designated Number of Degrees of Freedom, μ , for Various Partial Width Distributions | 21 |
| 4. Experimentally Evaluated Ta ¹⁸¹ Cross Sections in the Unresolved Resonance Range | 24 |
| 5. Selected Reference Data for Ta ¹⁸¹ Total Cross Section Measurements in the Unresolved Resonance Range. | 25 |
| 6. Zero Energy Parameters Extrapolated From Unresolved Resonance Energy-Dependent Parameter Fit | 26 |
| 7. Listing of Energy-Dependent Unresolved Resonance Parameters for Ta ¹⁸¹ | 28 |
| 8. Listing of Energy-Independent Unresolved Resonance Parameters for Ta ¹⁸¹ | 31 |
| 9. Fitted Smooth Background Cross Sections for Ta ¹⁸¹ | 31 |
| 10. Infinitely Dilute Resonance Integral for Capture in Ta ¹⁸¹ | 32 |
| 11. Comparison of Self-Shielding Factors for Ta ¹⁸¹ | 33 |
| 12. Infinitely Dilute Resonance Integral for Capture in Ta ¹⁸² | 33 |
| 13. Deformed Nucleus Optical Model Parameters | 35 |
| 14. Capture Model Parameters for Tantalum | 37 |
| 15. Level Diagrams for Tantalum Isotopes. | 37 |
| 16. Selected Reference Data for Ta ¹⁸¹ Total Cross Section Measurements Above 1 Mev. | 41 |

FIGURES

| | Page |
|---|------|
| 1. Calculated and Measured Neutron Cross Sections of Ta ¹⁸¹ Between 0.002 and 1.0 ev. | 12 |
| 2. Calculated and Measured Neutron Capture and Total Cross Sections of Ta ¹⁸² Between 0.01 and 3.0 ev | 14 |
| 3. Calculated Neutron Scattering Cross Sections of Ta ¹⁸² Between 0.01 and 3.0 ev. | 16 |
| 4. Unadjusted Capture Cross Section Data and Evaluated Curve for Ta ¹⁸¹ | 39 |
| 5. Unadjusted Total Cross Section Data and Evaluated Curve for Ta ¹⁸¹ | 43 |
| 6. Ta ¹⁸¹ Differential Elastic Scattering Cross Section (900 to 901 kev) | 46 |
| 7. Ta ¹⁸¹ Differential Elastic Scattering Cross Section (13.4 to 14.0 Mev). | 47 |
| 8. Inelastic Excitation of Ta ¹⁸¹ | 48 |
| 9. Ta ¹⁸¹ (n,α) and Ta ¹⁸¹ (n,nα) Measurements | 50 |
| 10. Evaluated Cross Sections for the Ta ¹⁸¹ (n,α) + Ta ¹⁸¹ (n,nα) Reaction. | 52 |
| 11. The Ta ¹⁸¹ (n,p) Hf ¹⁸¹ Reaction. | 53 |

ABSTRACT

Neutron cross section data for Ta¹⁸¹ and Ta¹⁸² have been evaluated at Atomics International for the ENDF/B library. Because of the lack of experimental data for Ta¹⁸², much of the information contained in the data set is based on theoretical calculations. A complete set of neutron cross section data was prepared for each nuclide for incident neutron energies between 10^{-5} ev and 17 Mev. These data, in ENDF/B format, are available from the National Neutron Cross Section Center at Brookhaven National Laboratory.

I. INTRODUCTION

An evaluation of available measured neutron cross section resonance parameters, differential angular distributions and other pertinent data for tantalum-181 and tantalum-182 has been completed. The need for reevaluating and updating the neutron cross sections for Ta^{181} originally prepared for the ENDF/B library was established by results of ENDF/B Phase II data testing. The evaluated data set for Ta^{182} constitutes the first ENDF/B evaluation made.

Measured cross section data were selected where available. Negative energy resonances were provided so as to match the low energy absorption and scattering cross sections. The evaluated resolved and unresolved resonance parameters were checked by comparing calculations of absorption cross sections and resonance integrals with available measured data. The agreement was satisfactory. Above 100 keV, the available measured data were augmented by theoretical calculations. Complete sets of neutron cross sections were calculated for each isotope, combined with the measured data where available, and the evaluated data sets produced.

II. EVALUATION OF CROSS SECTION DATA BELOW 100 kev

A. RESOLVED RESONANCE REGION

1. Evaluation Methods

Resolved resonance parameters derived from transmission measurements were evaluated for Ta^{181} and Ta^{182} . Missing values for radiation widths, Γ_γ , and compound nucleus spins, J , were supplied via theory. The set of resolved resonances was examined to determine: (1) the probable number of p-wave resonances which had been resolved and (2) the upper energy limit of resolution.

The potential scattering cross section was evaluated. Cross sections at thermal energies were calculated from the selected parameters and compared to measured values. Since the calculated thermal cross sections were smaller than measured values, parameters were determined for a negative energy resonance which would supply the additional thermal cross section contributions necessary to match the evaluation of measured values.

All resolved resonances in the evaluated set are assumed to be for s-wave ($\ell = 0$) neutrons. All suspected p-wave resonances were eliminated. The p-wave contributions in the resolved resonance range have been given as smooth background. However, the unresolved resonance parameters may be used to generate the p-wave contributions, and thus allow for resonance self-shielding. By eliminating p-wave resolved resonances and supplying all the p-wave cross sections from unresolved parameters (or smooth cross sections), it is more certain that the p-wave cross section is adequately represented.

2. Positive Energy Resolved Resonance Parameters

Values of E_0 , $2g\Gamma_n$, and Γ_γ are taken from BNL-325⁽¹⁾ for Ta^{181} . The value of $2g\Gamma_n$ for the 55.8 ev resonance was corrected to 0.2 mv. As shown in Reference 1, the values of $2g\Gamma_n$ are given by only one set of measurements above 248 ev.

Measured values of J for Ta^{181} are taken from Wasson 1969.⁽²⁾ J values are known for the 4.3, 10.3, 14.0, and 23.9 ev resonances. The resonances at 35.1 and 35.9 ev have been determined to have different J values. $J = 3$ was assigned to the 35.1 ev resonance and $J = 4$ to the 35.9 ev resonance.

Values of E_0 , $2g\Gamma_n$, and Γ_γ derived from measurements on Ta^{182} are taken from Stokes,⁽³⁾ which is the only data available. No measured values of J have been reported.

Ta^{181} and Ta^{182} have spin $I \neq 0$ so that two values of compound nucleus spin $J = I \pm 1/2$ are possible. For many resonances of the tantalum isotopes these values have not been established experimentally. Often resonances with unknown J values are assigned $J = I$ to form a third group. This approach may lead to serious errors when calculating thermal scattering cross sections, because interference between resonance and potential scattering is usually important in this calculation. The interference takes place between the potential scattering amplitude and the total resonance scattering amplitude of each set of resonances having a particular J value. Thus, if a third set of resonances is formed (whether or not they are allowed to interfere with potential scattering) the calculation will be in error.

The procedure used in this evaluation was to assign a possible J value to each resonance so that the potential scattering interferes with more nearly correct resonance scattering terms. The J values were assigned in proportion to $(2J + 1)$ as given by theory. (This division is less sophisticated than that used for determining the unresolved resonance level spacings but appears to be adequate for this purpose.)

The value of Γ_n was changed to preserve the experimentally determined values of $2g\Gamma_n$ in all cases except for the three lowest energy resonances of Ta^{182} . For these, the peak cross section $\propto (g\Gamma_n/\Gamma)$ was preserved because shape analysis, rather than area analysis, had been used to derive their parameters. The total width is nearly preserved in these cases because $\Gamma_n \ll \Gamma$.

For resonances with unknown radiation widths an average value of Γ_γ was used. The arithmetic average of the 26 resolved values for Ta^{181} , 56 mv, was used. This value is lower than that obtained for the unresolved resonance range. The capture resonance integral calculated using 56 mv for the unknown resonances is in good agreement with the evaluated value (see Table 10). The capture width of Ta^{182} is reported for only three resonances. The value of 67 mv found for all three was used for the other resolved resonances.

3. Upper Energy Limit of Resolved Resonance Range

In general, experimental resolution decreases with increasing energy while average total widths of resonances increase with energy. Because the decrease in experimental resolution is dominant, a smaller percentage of resonances are resolved as energy increases. At sufficiently high energies, experiments miss some of the smaller s-wave resonances. Resolution of a "resonance" which is really only a statistical fluctuation in the data is a further consideration. It is probably important only at energies where a large number of s-wave resonances are missed. When the number of resolved resonances below a given energy is plotted vs energy, a generally convex function is expected. Typically, these functions behave linearly over a fairly large energy range. This linearity indicates that all the s-wave but none of the p-wave resonances have been resolved. The high energy end of the linear region may be taken as the limit of identification of all s-wave resonance energies.

For Ta¹⁸¹ the upper end of the linear region coincides with the energy below which all observed s-wave resonances have resolved values of Γ_n . This occurs about 330 ev, and the limit is taken there. For Ta¹⁸² the small number of resonances resolved and the obscuring of energy regions by resonances of other isotopes in the measured samples make the above analysis inapplicable. The resolved range was set to include all resonances with resolved values of Γ_n . Unfortunately, a large resonance exists at 34.7 ev, just above the resolved range.

4. p-Wave Resolved Resonances

If the linear portion of the level density plot is extended to the ordinate axis, the intercept is a measure of the number of p-wave resonances resolved. For Ta¹⁸¹ the intercept was zero indicating no resolved p-wave resonances.

More sophisticated analyses to estimate the number of missed s-wave resonances and resolved p-wave resonances are possible. These methods use known resolution functions, statistical distributions of level widths, and evaluated strength functions. Because the χ^2 distribution with one degree of freedom is broad, a large number of resolved Γ_n values are needed to profitably use those methods. Their use for Ta¹⁸¹ would probably be marginal with the current data.

For Ta¹⁸² no resonances of very small width were resolved, so all resolved resonances were assumed to be s-wave resonances.

5. Potential Scattering Cross Section

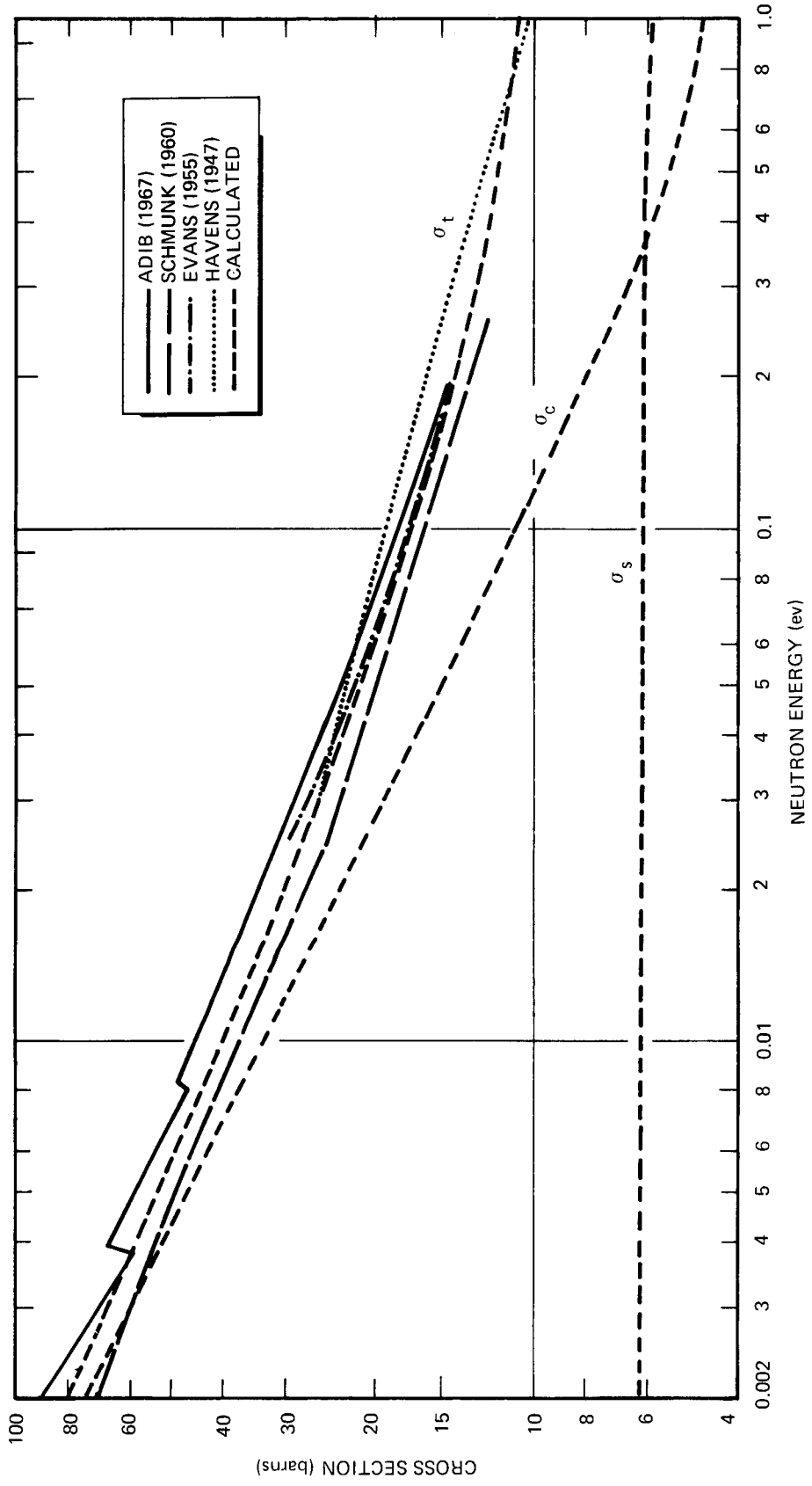
Seth⁽⁴⁾ determined the potential scattering cross section of natural tantalum to be 8.5 ± 0.8 barns by subtracting calculated resonance contributions from measured total cross sections in the low energy resolved resonance range, and by transmission analysis in the kev range. The total cross section at 100 kev using the latter value is about 0.2 barn higher than the evaluated experimental cross section of 9.0 ± 0.9 barns. The comparison at 100 kev is a good test because potential scattering contributes over 80% of the total cross section, which is known to be $\pm 10\%$. The value of 8.3 ± 0.8 barns was adopted for both tantalum isotopes. This value fits well an interpolation of measured potential scattering cross sections vs atomic mass near $A = 180$.⁽⁵⁾

6. Thermal Cross Sections and Negative Energy Resonances

Cross sections near thermal energies are generally better known than at higher energies. They provide a good control for values calculated from resonance parameters. If values calculated from positive energy resonances are too high, the most likely error is that one or more level widths of a large resonance are incorrect. Usually, a single resonance provides the majority of the capture cross section well below the lowest energy resonance. By adjusting the parameters of only that resonance, a good fit to measured values can often be obtained.

If calculated values are too low, level widths may be in error, as above, or one or more negative energy levels may be indicated. The accuracy to which the measured cross sections are known does not permit the determination of parameters for more than one resonance. Occasionally a choice between adjusting positive energy resonance parameters and introduction of a negative energy resonance can be made by comparisons with resonance integrals and/or the cross section minima between low lying positive energy resonances. Usually the choice is somewhat arbitrary. A single negative energy resonance was introduced for this evaluation.

The multilevel scattering interference formulation was used to derive the negative energy resonance parameters, and to calculate cross sections for comparison to experiment. Its use is particularly important for calculating the low



7762-4646

Figure 1. Calculated and Measured Neutron Cross Sections of Ta¹⁸¹
Between 0.002 and 1.0 eV

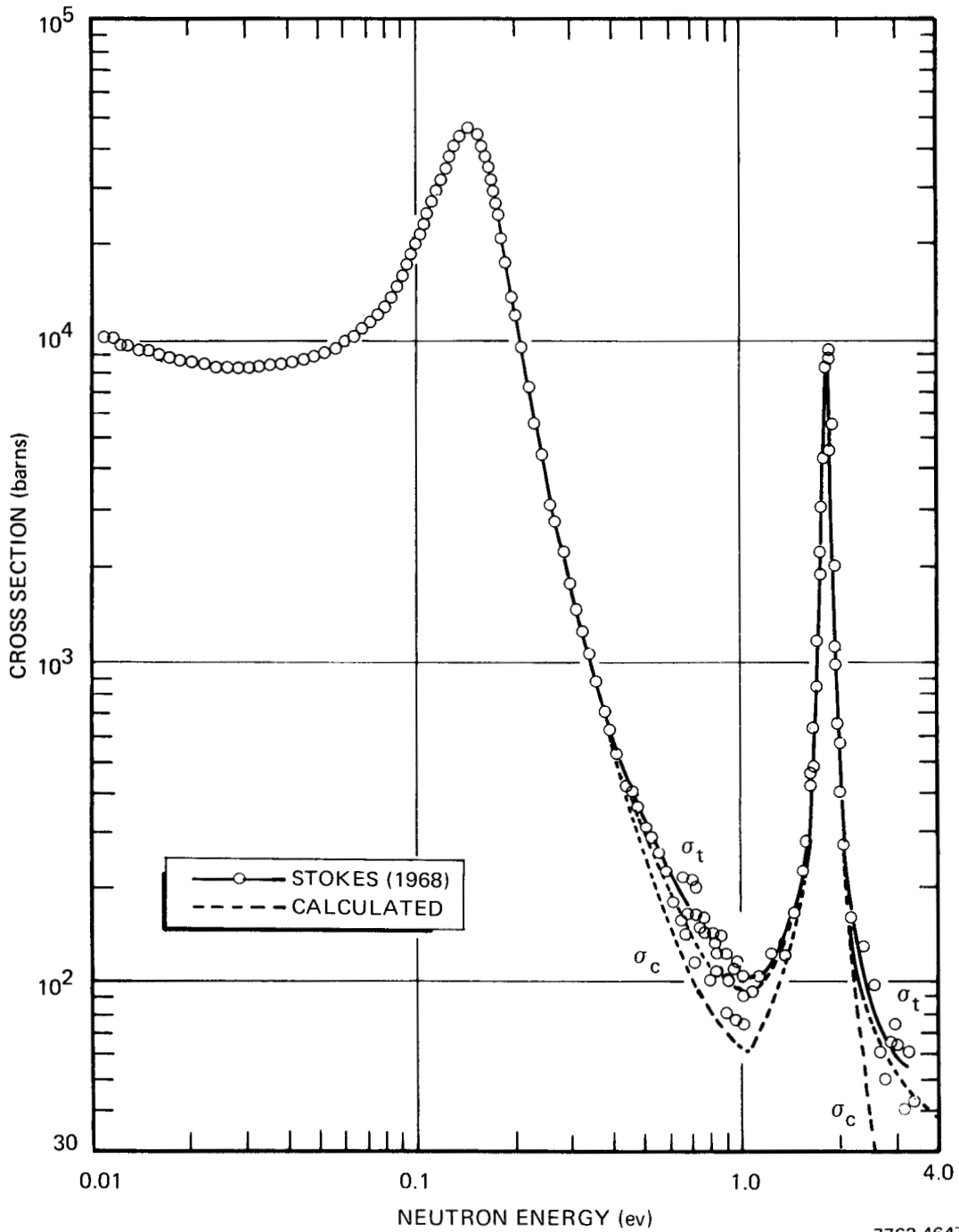
energy scattering cross sections.⁽⁶⁾ The UNICORN⁽⁷⁾ code was used to make the calculations.

Experimental values of the total cross section for Ta¹⁸¹ below 1 ev are taken from Havens,⁽⁸⁾ Evans,⁽⁹⁾ Schmunk,⁽¹⁰⁾ and Adib.⁽¹¹⁾ They are shown in Figure 1. The total cross section at 0.0253 ev was evaluated to be 28 ± 3 barns. The evaluated capture cross section at 0.0253 ev of 21 ± 3 barns was taken from BNL-325.⁽¹⁾ Cross sections calculated from the positive energy resonance parameters were $\sigma_c = 16.3$ barns and $\sigma_t = 21.4$ barns.

If the 0.0253 ev discrepancies were to be accounted for by adjustment of the 4.3 ev resonance capture width, the revised width would be improbably large and the total cross section too small. If the scattering width of the 4.3 ev resonance were revised, disagreement with the measured capture resonance integral would result. Thus, the discrepancies were attributed to negative energy resonances.

The parameters for a negative energy resonance were determined by fitting the evaluated capture and total 2200 m/s cross sections. The fit was obtained by an iterative procedure (necessary because of scattering interference) which was terminated before exact agreement was obtained, as justified by the experimental uncertainties. Γ_γ was fixed at its average value and Γ_n and E_0 allowed to vary. The spin assignment made little difference when the variable parameters were independently optimized. The calculated values of σ_c , σ_s , and σ_t between 0.01 and 1.0 ev are shown in Figure 1. The 2200 m/s cross sections calculated from all resonances are $\sigma_c = 21.1$ barns, $\sigma_s = 6.2$ barns, and $\sigma_t = 27.3$ barns. The scattering cross section is in good agreement with the value of 6 barns recommended by Hughes.⁽¹²⁾

The only data for Ta¹⁸² is that of Stokes⁽³⁾ who gives a 2200 m/s total cross section of 8200 ± 600 barns. The value calculated from positive energy resolved resonances is 8215 barns. The other spin assignment for the 0.147 ev resonance would change this value by +20 barns. At 1 and 3 ev, which are near minima in the local cross section, the calculated total cross sections are about 30 barns less than the measured values. These calculated values are affected little by spin assignments. The presence of a negative energy level is thus indicated.



7762-4647

Figure 2. Calculated and Measured Neutron Capture and Total Cross Sections of Ta^{182} Between 0.01 and 3.0 eV

A negative energy level was created with Γ_γ chosen to be the average radiation width and the resonance energy, E_0 taken to be -20 ev, which is small enough to give an approximately $1/v$ capture cross section below 1 ev, i.e., $|E_0/2| \gg 1$. The neutron width was calculated to give $\sigma_t = 29$ barns at 1 ev.

The comparison between the measured and calculated capture and total cross sections below 3 ev is shown in Figure 2. The calculated 2200 m/s cross sections are $\sigma_c = 8249$ barns, $\sigma_s = 31$ barns, and $\sigma_t = 8280$ barns. The choice of negative energy resonance parameters and spin assignments for resonances may vary the scattering cross section considerably. Below 0.4 ev it is estimated to be known only to about $\pm 75\%$. The effect of choice of spin assignments for the negative energy resonance is shown in Figure 3.

7. Tabulation of Resonance Parameters

As a result of the evaluations discussed in Sections II-A-2 and -6, a set of resonance parameters were obtained for the ENDF/B evaluation. Table 1 presents the data for Ta¹⁸¹ (MAT 1126) and Table 2 presents the data for Ta¹⁸² (MAT 1127).

B. UNRESOLVED RESONANCE REGION

1. Methods of Evaluation

The unresolved resonance parameters were determined by a combination of theoretical assumptions and fits to evaluated measured cross sections. Theory had to be invoked to limit the number of independent variables, because the accuracy of the measured cross sections was only sufficient to determine a few variables unambiguously.

Two types of fits were made. For the convenience of those without computer codes which accommodate energy-dependent parameters, a fit with energy-independent parameters was given for the ENDF/B.

The following assumptions were made for the energy-independent fit:

- 1) The radiation level width is independent of energy, neutron angular momentum l , and compound nucleus spin J .

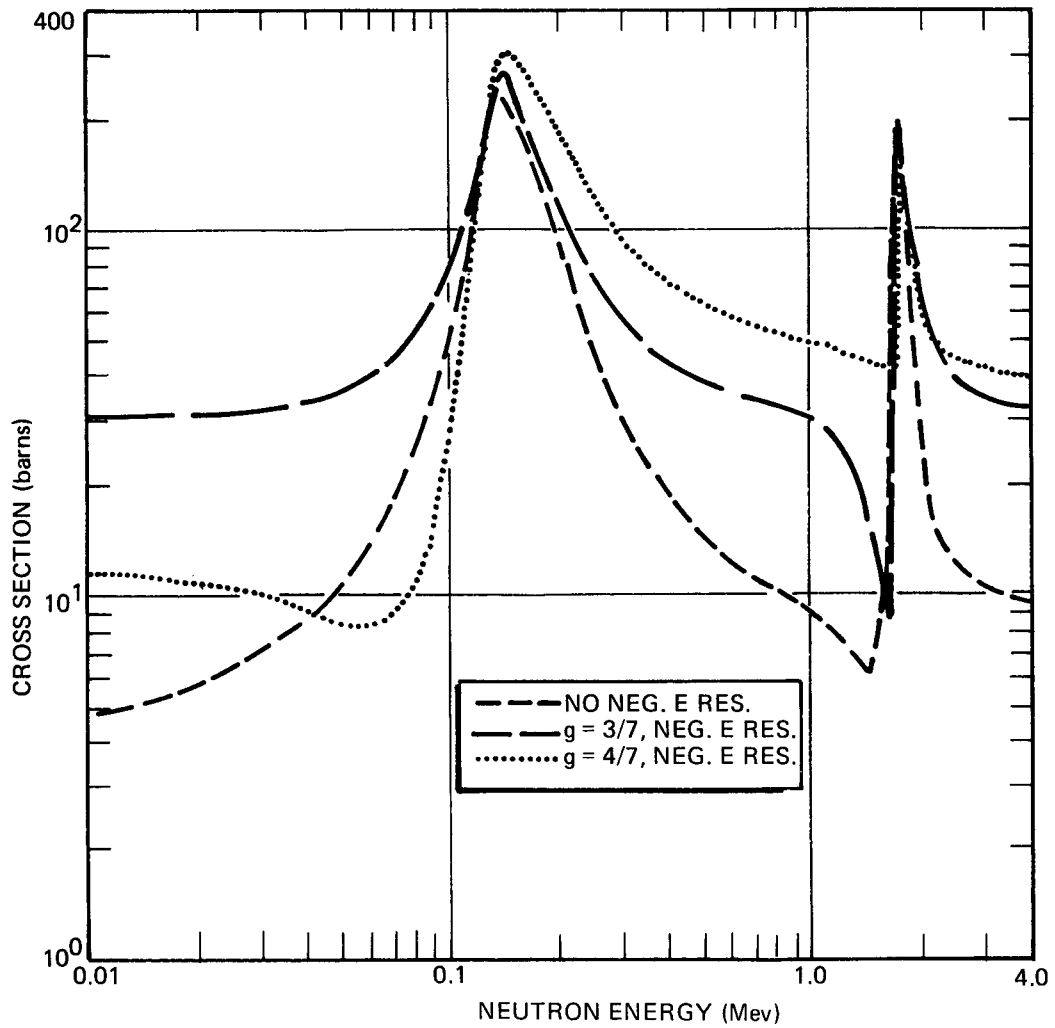


Figure 3. Calculated Neutron Scattering Cross Sections of Ta^{182} Between 0.01 and 3.0 ev

TABLE 1
RESOLVED RESONANCE PARAMETERS FOR Ta¹⁸¹
(Sheet 1 of 2)

| Number | Energy (ev) | Neutron Width (ev) | Radiation Width (ev) | Statistical Weight |
|--------|----------------|--------------------------|-------------------------|--------------------|
| 1 | -14.4 | 0.375 x 10 ⁻¹ | 0.056 | 0.4375 |
| 2 | 4.28 | 0.390 x 10 ⁻² | 0.053 | 0.5625 |
| 3 | 10.34 | 0.466 x 10 ⁻² | 0.055 | 0.4375 |
| 4 | 13.95 | 0.101 x 10 ⁻² | 0.052 | 0.5625 |
| 5 | 20.30 | 0.102 x 10 ⁻² | 0.060 | 0.5625 |
| 6 | 22.70 | 0.251 x 10 ⁻³ | 0.052 | 0.4375 |
| 7 | 23.90 | 0.743 x 10 ⁻² | 0.053 | 0.4375 |
| 8 | 30.00 | 0.196 x 10 ⁻³ | 0.055 | 0.5625 |
| 9 | 35.16 | 0.121 x 10 ⁻¹ | 0.065 | 0.4375 |
| 10 | 35.90 | 0.150 x 10 ⁻¹ | 0.065 | 0.5625 |
| 11 | 39.13 | 0.512 x 10 ⁻¹ | 0.060 | 0.4375 |
| 12 | 49.15 | 0.933 x 10 ⁻³ | 0.053 | 0.5625 |
| 13 | 55.80 | 0.229 x 10 ⁻³ | 0.056 | 0.4375 |
| 14 | 57.54 | 0.231 x 10 ⁻³ | 0.056 | 0.5625 |
| 15 | 59.05 | 0.137 x 10 ⁻³ | 0.056 | 0.4375 |
| 16 | 63.12 | 0.516 x 10 ⁻² | 0.064 | 0.5625 |
| 17 | 76.85 | 0.137 x 10 ⁻¹ | 0.048 | 0.4375 |
| 18 | 77.64 | 0.498 x 10 ⁻² | 0.054 | 0.5625 |
| 19 | 78.95 | 0.194 x 10 ⁻² | 0.056 | 0.4375 |
| 20 | 82.94 | 0.124 x 10 ⁻¹ | 0.052 | 0.5625 |
| 21 | 85.10 | 0.469 x 10 ⁻² | 0.058 | 0.4375 |
| 22 | 85.75 | 0.178 x 10 ⁻³ | 0.056 | 0.5625 |
| 23 | 89.60 | 0.293 x 10 ⁻² | 0.055 | 0.5625 |
| 24 | 91.44 | 0.204 x 10 ⁻² | 0.056 | 0.5625 |
| 25 | 97.00 | 0.366 x 10 ⁻² | 0.056 | 0.4375 |
| 26 | 99.32 | 0.102 x 10 ⁰ | 0.050 | 0.5625 |
| 27 | 103.52 | 0.126 x 10 ⁻² | 0.056 | 0.4375 |
| 28 | 105.54 | 0.267 x 10 ⁻¹ | 0.050 | 0.5625 |
| 29 | 115.08 | 0.469 x 10 ⁻¹ | 0.057 | 0.4375 |
| 30 | 118.32 | 0.213 x 10 ⁻² | 0.056 | 0.5625 |
| 31 | 126.46 | 0.503 x 10 ⁻¹ | 0.054 | 0.4375 |
| 32 | 136.48 | 0.196 x 10 ⁻¹ | 0.047 | 0.5625 |
| 33 | 138.33 | 0.149 x 10 ⁻¹ | 0.066 | 0.4375 |
| 34 | 144.21 | 0.160 x 10 ⁻² | 0.056 | 0.5625 |
| 35 | 148.31 | 0.526 x 10 ⁻² | 0.056 | 0.4375 |
| 36 | 149.70 | 0.489 x 10 ⁻² | 0.056 | 0.5625 |
| 37 | 159.80 | 0.343 x 10 ⁻³ | 0.056 | 0.4375 |
| 38 | 166.40 | 0.756 x 10 ⁻² | 0.056 | 0.5625 |

TABLE 1
RESOLVED RESONANCE PARAMETERS FOR Ta¹⁸¹
(Sheet 2 of 2)

| Number | Energy (ev) | Neutron Width (ev) | Radiation Width (ev) | Statistical Weight |
|--------|-------------|------------------------|----------------------|--------------------|
| 39 | 175.00 | 0.889×10^{-1} | 0.056 | 0.5625 |
| 40 | 176.00 | 0.587×10^{-1} | 0.056 | 0.5625 |
| 41 | 178.60 | 0.114×10^{-2} | 0.056 | 0.4375 |
| 42 | 182.80 | 0.844×10^{-3} | 0.056 | 0.5625 |
| 43 | 185.50 | 0.686×10^{-3} | 0.056 | 0.4375 |
| 44 | 189.30 | 0.622×10^{-3} | 0.056 | 0.5625 |
| 45 | 194.80 | 0.128×10^0 | 0.056 | 0.4375 |
| 46 | 200.00 | 0.356×10^{-1} | 0.062 | 0.5625 |
| 47 | 204.70 | 0.297×10^{-2} | 0.056 | 0.4375 |
| 48 | 208.40 | 0.978×10^{-2} | 0.056 | 0.5625 |
| 49 | 215.00 | 0.549×10^{-1} | 0.065 | 0.4375 |
| 50 | 216.60 | 0.160×10^{-1} | 0.056 | 0.5625 |
| 51 | 219.70 | 0.191×10^{-1} | 0.056 | 0.4375 |
| 52 | 222.30 | 0.196×10^{-2} | 0.052 | 0.5625 |
| 53 | 225.30 | 0.257×10^{-1} | 0.056 | 0.4375 |
| 54 | 230.50 | 0.160×10^{-1} | 0.056 | 0.5625 |
| 55 | 232.30 | 0.578×10^{-1} | 0.056 | 0.5625 |
| 56 | 237.30 | 0.124×10^{-2} | 0.056 | 0.5625 |
| 57 | 242.70 | 0.111×10^{-1} | 0.056 | 0.4375 |
| 58 | 247.20 | 0.560×10^{-2} | 0.056 | 0.5625 |
| 59 | 248.40 | 0.160×10^{-2} | 0.056 | 0.4375 |
| 60 | 253.00 | 0.267×10^{-3} | 0.056 | 0.5625 |
| 61 | 259.10 | 0.126×10^{-1} | 0.056 | 0.4375 |
| 62 | 263.30 | 0.844×10^{-1} | 0.056 | 0.5625 |
| 63 | 264.70 | 0.160×10^{-1} | 0.056 | 0.4375 |
| 64 | 271.80 | 0.124×10^{-1} | 0.056 | 0.5625 |
| 65 | 273.90 | 0.114×10^0 | 0.056 | 0.4375 |
| 66 | 277.20 | 0.222×10^{-1} | 0.056 | 0.5625 |
| 67 | 280.30 | 0.343×10^{-1} | 0.056 | 0.4375 |
| 68 | 287.70 | 0.240×10^{-1} | 0.056 | 0.5625 |
| 69 | 290.40 | 0.229×10^{-1} | 0.056 | 0.4375 |
| 70 | 291.10 | 0.889×10^{-2} | 0.056 | 0.5625 |
| 71 | 304.00 | 0.240×10^{-2} | 0.056 | 0.5625 |
| 72 | 306.20 | 0.276×10^{-1} | 0.056 | 0.5625 |
| 73 | 311.70 | 0.286×10^{-1} | 0.056 | 0.4375 |
| 74 | 313.30 | 0.356×10^{-1} | 0.056 | 0.5625 |
| 75 | 322.80 | 0.686×10^{-2} | 0.056 | 0.4375 |
| 76 | 329.40 | 0.400×10^{-1} | 0.056 | 0.5625 |

TABLE 2
RESOLVED RESONANCE PARAMETERS FOR Ta¹⁸²

| Number | Energy (ev) | Neutron Width (ev) | Radiation Width (ev) | Statistical Weight |
|--------|-------------|--------------------------|----------------------|--------------------|
| 1 | -20.0 | 0.630 × 10 ⁰ | 0.067 | 0.42857 |
| 2 | 0.147 | 0.315 × 10 ⁻³ | 0.067 | 0.57143 |
| 3 | 1.82 | 0.135 × 10 ⁻² | 0.067 | 0.42857 |
| 4 | 5.98 | 0.406 × 10 ⁻³ | 0.067 | 0.57143 |
| 5 | 12.93 | 0.671 × 10 ⁻³ | 0.067 | 0.42857 |
| 6 | 21.50 | 0.142 × 10 ⁻² | 0.067 | 0.57143 |
| 7 | 26.66 | 0.392 × 10 ⁻² | 0.067 | 0.42857 |
| 8 | 29.40 | 0.133 × 10 ⁻² | 0.067 | 0.57143 |
| 9 | 32.97 | 0.134 × 10 ⁻¹ | 0.067 | 0.42857 |
| 10 | 34.65 | 0.300 × 10 ⁻² | 0.067 | 0.57143 |

2) The strength functions,

$$S_{\ell,J} = \frac{\langle \Gamma_n^0 \rangle_{\ell,J}}{\langle D \rangle_{\ell,J}},$$

are independent of J and energy E.

3) The average level spacing $\langle D \rangle_{\ell,J}$ is independent of ℓ and energy, and its J dependence is given by the formula of Cook;⁽¹³⁾ namely,

$$\langle D \rangle_J \propto (2J+1)^{-1} \exp \left[-\frac{\left(J+\frac{1}{2}\right)^2}{2\sigma^2} \right],$$

where σ is a constant for each isotope.

4) Elastic scattering with a change of ℓ value and inelastic scattering are neglected. This assumption is necessary because the ENDF/B format does not allow for these processes explicitly.

5) Doubly occurring (ℓ, J) series were assumed to be single series with two degrees of freedom rather than two competing series each with one degree of freedom. The former is easier to accommodate in the current ENDF/B format and the practical difference is negligible.

A second, more accurate fit was made without invoking assumption 4 above, and with the energy dependence of $\langle D \rangle_{\ell,J}$ given by Cook et al.⁽¹³⁾ The strength functions for inelastic scattering were assumed to be the same as for elastic scattering.

Smooth background cross sections were supplied (ENDF/B File 3) to match evaluated results for both the energy-dependent and energy-independent fits.

The radius "a" of the centrifugal potential well used to calculate angular momentum barrier penetration probabilities for neutrons with non-zero angular momenta was taken equal to $\left[1.23 (A/m_n)^{1/3} + 0.8\right]$ fermis as required by ENDF/B.

The calculation of average cross sections from resonance parameters involves averaging over the distributions of reaction level widths. This is often done by combining a "fluctuation integral" $R_{i\ell,J}$ with cross sections calculated from average widths.

$$R_{i\ell,J} = \frac{\left\langle \frac{\Gamma_n \Gamma_i}{\Gamma} \right\rangle_{\ell,J}}{\left(\frac{\bar{\Gamma}_{n\ell,J} \bar{\Gamma}_{i\ell,J}}{\bar{\Gamma}_{\ell,J}} \right)}$$

In calculating $R_{i\ell,J}$, a χ^2 distribution with $\mu_{i\ell,J}$ degrees of freedom is assumed. In addition, $\mu_{n\ell,J}$ is used to obtain $\bar{\Gamma}_{n\ell,J}$ from the input $\bar{\Gamma}_{n\ell,J}^0$:

$$\bar{\Gamma}_{n\ell,J} = \bar{\Gamma}_{n\ell,J}^0 \mu_{n\ell,J} \nu_\ell \sqrt{E}$$

where ν_ℓ is the angular momentum barrier penetration factor.

The values of $\mu_{i\ell,J}$ for the competitive reaction width and elastic scattering are given in Table 3. For all ℓ and J , $\mu_{\gamma\ell,J}$ is assumed to be infinite, i.e., the radiation width $\Gamma_{\gamma\ell,J}$ is constant.

The remaining independent variables include the potential scattering cross section, σ_{pot} , the average radiation width $\langle \Gamma_\gamma \rangle$, the strength functions, and $\langle D \rangle_{\ell,J}$ for one (ℓ,J) series. In practice, the $\ell = 0$ level spacing, $\langle D \rangle_{\ell=0}$, was used.

The unresolved resonance parameters were ultimately determined by minimizing the goodness-of-fit between calculated and evaluated (described later) capture cross sections. The uncertainty in evaluated cross sections was assumed to be independent of energy. Fitting was done with a computer program⁽¹⁴⁾ which

TABLE 3
DESIGNATED NUMBER OF DEGREES OF FREEDOM, μ , FOR
VARIOUS PARTIAL WIDTH DISTRIBUTIONS

| Isotope | Angular Momentum, l | Compound Nucleus Spin, J | μ_n for Neutron Widths | μ_x for Competitive Reaction Widths |
|-------------------|-----------------------|----------------------------|----------------------------|---|
| Ta ¹⁸¹ | 0 | 3 | 1 | 1 |
| | 0 | 4 | 1 | 2 |
| | 1 | 2 | 1 | 1 |
| | 1 | 3 | 2 | 2 |
| | 1 | 4 | 2 | 1 |
| | 1 | 5 | 1 | 1 |
| | 2 | 1 | 1 | - |
| | 2 | 2 | 2 | - |
| | 2 | 3 | 2 | 1 |
| | 2 | 4 | 2 | 2 |
| | 2 | 5 | 2 | 2 |
| | 2 | 6 | 1 | 2 |
| | Ta ¹⁸² | 0 | 5/2 | 1 |
| 0 | | 7/2 | 1 | - |
| 1 | | 3/2 | 1 | - |
| 1 | | 5/2 | 2 | - |
| 1 | | 7/2 | 2 | - |
| 1 | | 9/2 | 1 | - |

minimizes χ^2 by using a grid search and iteration procedure. The search is made on $\langle D \rangle_{l=0}$, $\langle \Gamma_\gamma \rangle$, S_0 , S_1 , and S_2 , in that order. The code uses the resonance treatment of the TRIX⁽¹⁵⁾ code, which makes the isolated resonance approximation and accounts for level width distributions by averaging integrals over statistical samples. The starting values for the search were taken from averages over the resolved resonances plus estimates for S_1 and S_2 .

2. Energy Range for Unresolved Resonances Region

Very large lumps of tantalum have been proposed for reflector poison-backings of compact reactors and control rods of fast breeder reactors. The combination of the high importance at high energies and the large lump sizes cause resonance self-shielding to have significant reactivity effects at unusually high energies. Consequently, the upper limit of the unresolved energy range has been set at 100 keV for Ta¹⁸¹. For high temperatures this may be unnecessarily high because of overlapping of resonances due to Doppler broadening. However, it is easier to transform resonance parameters into smooth cross sections than vice versa.

Ta^{182} is almost always combined with Ta^{181} , but is normally present at low concentrations. Self-shielding for Ta^{182} is a factor only at low energy where the optical dimension is significant. For this reason the unresolved resonance high energy limit has been set at 10 kev. Smooth cross sections generated from resonance parameters have been supplied from 10 to 100 kev.

s-, p-, and d-wave neutrons contribute significantly to reaction rates over different restricted energy ranges. p-wave contributions to capture are less than 0.2% of the total below 330 ev, and d-wave contributions less than 0.1% below 10 kev. Two energy ranges were made for unresolved resonances in Ta^{181} . From 330 ev to 10 kev, only s- and p-wave contributions were calculated and from 10 to 100 kev, s-, p-, and d-wave contributions were all calculated. Since the upper energy limit of the unresolved range for Ta^{182} is 10 kev, no d-wave calculation was made, and a single unresolved energy range was used, namely, 35 ev to 10 kev.

In general, since the resolved resonance range contains only s-wave resonances, some contribution from unresolved p-wave resonances is called for. However, as noted previously, these contributions are negligible for tantalum.

3. Average Parameters Derived From Resolved Resonances

a. Ta^{181}

The s-wave strength function determined from the resolved resonance data is $S_0 = (1.8 \pm 0.4) \times 10^{-4}$, $\langle \Gamma_\gamma \rangle = 56 \pm 2$ mv, and $\langle D \rangle_{\ell=0} = 4.4 \pm 0.5$ ev. $\langle \Gamma_\gamma \rangle$ was obtained by an unweighted average of the 26 measured values. The distribution of values conformed closely to a normal distribution and was unusually narrow.

b. Ta^{182}

The s-wave strength function of 1.0×10^{-4} is based upon 8 resonances and is thus not very helpful. It is apparent from the data of Stokes⁽³⁾ that the value is considerably larger in the region adjacent to the resolved resonance range. All three measured values of Γ_γ are the same, 67 mv, with $\langle D \rangle_{\ell=0} = 3.5 \pm 1.2$ ev. Since a good test against measured cross sections was not possible, $\langle \Gamma_\gamma \rangle = 67$ mv and $\langle D \rangle_{\ell=0} = 3.5$ ev were adopted for the unresolved resonance range.

4. Experimental Data Evaluation for Unresolved Resonance Energy Range

a. Radiative Capture Cross Section

From the upper bound of the resolved resonance region, 330 ev, to 1 kev three sets of (n,γ) data in Ta^{181} are available. Block et al⁽¹⁶⁾ at Oak Ridge (1961) detected gammas with a liquid scintillator tank; Moxon and Rae⁽¹⁷⁾ at Harwell (1963) detected gammas with a plastic scintillator (Moxon-Rae counter); and Konks⁽¹⁸⁾ at the Lebedev Institute (1963) used a spectrometer based on the neutron slowing down time in lead (Figure 4).

The Harwell experiment yielded high resolution data. Because of this resolution their data were smoothed by averaging every 20 data points. This provided a curve which could be more easily compared to the other experiments.

Of the three data sets in this energy range, the Harwell and Lebedev Institute data agreed most closely, with the former slightly on the low side (as observed throughout this study for Moxon-Rae counter measurements). Consequently, these two sets were favored in the unresolved fit.

From 1 to 10 kev the liquid scintillator data of Fricke et al⁽¹⁹⁾ compared quite closely with the Harwell data providing a smooth curve to which the unresolved parameters could be fit. The Oak Ridge and Lebedev Institute results were higher in this range.

Above 10 kev we find reference to a large number of experiments. Between 10 and 50 kev the unresolved fit was made to the data of five experiments: Fricke et al, more recent data of Moxon (Harwell, 1968),⁽²⁰⁾ the time-of-flight data of Macklin and Gibbons,⁽²¹⁾ the Karlsruhe data of Kompe,⁽²²⁾ and the activation data of Brzosko.⁽²³⁾

In this energy range the data of Konks appears high just as it did below this range. The activation measurements of Booth,⁽²⁴⁾ Bergqvist,⁽²⁵⁾ and Miskel⁽²⁶⁾ are also all higher. This agrees with the general trend of earlier activation measurements observed throughout these studies. The liquid scintillation experiments of Gibbons et al,⁽²⁷⁾ Macklin et al,⁽²⁸⁾ and Kononov et al⁽²⁹⁾ also take place in this range. These measurements suffer from one fault; they have been normalized to the indium (n,γ) cross section measurements made in 1961 which are erroneous on the low side. Upon renormalization these data come into much better agreement with the selected data in this energy range on up to 160 kev.

Above 50 keV there is a divergence of data. Fricke's⁽¹⁹⁾ measurements level off with increasing energy to a value 0.46 barn at 100 keV. In contrast Kompe's⁽²²⁾ measurement indicates a 100 keV value of less than 0.40 barn. Between 95 and 110 keV, no other consistent measurements have been made. The renormalized activation measurements discussed above tend to support the lower value at 100 keV. Looking on both sides of this interval, the activation measurements of Booth⁽²⁴⁾ and Miskel⁽²⁶⁾ tend to support the lower value, while the activation results of Brzosko support an intermediate value. Consequently, a value 0.41 barn was adopted for the unresolved fit at 100 keV. Figure 4 in Section III shows a plot of the Ta¹⁸¹ capture cross section data and the final evaluated curve. Data for the references quoted above may be found in this figure. Table 4 shows the final values of capture cross section that were used in the unresolved resonance parameter fits described in Section II-B-4.

TABLE 4
EXPERIMENTALLY EVALUATED Ta¹⁸¹ CROSS SECTIONS
IN THE UNRESOLVED RESONANCE RANGE

| Energy (keV) | σ_t (b) | σ_c (b) |
|-----------------|-------------------|-------------------|
| 100 | 9.0 ± 0.9 | 0.41 ± 0.04 |
| 50 | 10.0 ± 1.5 | 0.61 ± 0.06 |
| 20 | 11.5 ± 2.3 | 1.10 ± 0.11 |
| 10 | 13.0 ± 2.6 | 1.75 ± 0.18 |
| 5 | 14.5 ± 2.9 | 2.70 ± 0.27 |
| 2 | 18.0 ± 3.6 | 5.60 ± 0.84 |
| 1 | 22.5 ± 4.5 | 10.0 ± 1.5 |
| 0.6 | 30.0 ± 6.0 | 14.5 ± 2.2 |
| 0.3 | 38.0 ± 7.6 | 20.0 ± 4.0 |

b. Total Cross Section

Much of the total cross section data for Ta¹⁸¹ between 330 eV and 100 keV are considerably dated. Table 5 indicates the references which were used in evaluating the total cross section in the unresolved resonance region (Figure 5).

Most of these data are quite oscillatory reflecting the resonance nature of this region. To represent these data with unresolved resonance parameters, a

TABLE 5
 SELECTED REFERENCE DATA FOR Ta¹⁸¹ TOTAL
 CROSS SECTION MEASUREMENTS IN THE UNRE-
 SOLVED RESONANCE ENERGY RANGE

| Author | Laboratory | Year | Energy Range | Reference |
|---------------------------|-------------------------|------|----------------|-----------|
| C. K. Bockelman et al | University of Wisconsin | 1949 | 20 to 1600 kev | 30 |
| V. V. Vladimirovski et al | USSR | 1955 | 8 ev to 1 kev | 31 |
| H. W. Newson et al | Duke | 1957 | 2 to 6 kev | 32 |
| R. H. Tabony et al | Duke | 1965 | 30 to 650 kev | 33,34 |
| H. Camarda et al | Columbia | 1970 | 1 ev to 50 kev | 35 |

large number of points were averaged in a given experiment. The best smooth curve was used for parameter fits. Of the different experiments listed in Table 5, the 1970 Columbia University experiment was most extensive and included some 8000 data points.⁽³⁵⁾ These data were not on the SCISRS files but were obtained recently from Columbia University. They represent a major addition to the Ta¹⁸¹ total cross section data file. Figure 5 in Section III shows a plot of the Ta¹⁸¹ total cross section data and the final evaluated curve. Data for the references quoted above may be found in this figure. Table 4 shows the final values of total cross section that were used in the unresolved resonance parameter fits described in Section II-B-4.

The only measured data for Ta¹⁸² are the total cross section data of Stokes,⁽³⁾ which extend to only 1100 ev. The data are complicated by contributions from contaminants. Theory was relied upon for Ta¹⁸² in the unresolved resonance region.

A notable feature of Stokes data is a particularly large resonance at 34.7 ev just above the last resolved resonance at 32.97 ev. Resolved resonance parameters were derived for this resonance in order to give it a better representation.

The resolution is such that the resonance should be considered only partially resolved.

5. Parameter Fits to Experimental Data

a. Energy-Dependent Parameter Fit

The energy-dependent parameter fit to the capture cross section data for Ta¹⁸¹ shown in Table 4 yielded the parameters at zero energy in Table 6.

TABLE 6
ZERO ENERGY PARAMETERS EXTRAPOLATED
FROM UNRESOLVED RESONANCE ENERGY-
DEPENDENT PARAMETER FIT

| Parameter | Value | Uncertainty in Fit (%) |
|-----------------------------------|-----------------------|------------------------|
| $\langle D \rangle_{\ell=0}$ | 3.933 ev | 17 |
| $\langle \Gamma_{\gamma} \rangle$ | 65.1 mv | 30 |
| S_0 | 1.55×10^{-4} | 39 |
| S_1 | 0.72×10^{-4} | 126 |
| S_2 | 0.40×10^{-4} | 1650 |

The fit gives a χ^2 value of 2.2 assuming a 10% uncertainty in the fitted cross sections. This is well below the number of points minus parameters which is 4, indicating a good fit. $\langle D \rangle_{\ell=0}$ and S_0 agree adequately with values from the resolved resonance range. $\langle \Gamma_{\gamma} \rangle$ is considerably different although within the combined uncertainties. The value is closer to those of neighboring tungsten isotopes and not unreasonable.

Calculations using the fit from capture data do not give a particularly good fit to the evaluated total cross section, especially below 5 kev. The total cross section is not known as well, but the discrepancies appear to be comparable to the experimental uncertainty at some points. The calculated cross section is consistently too large by up to 27%. The smooth cross section file was used to eliminate the discrepancy.

The ENDF/B format accommodates only one competitive reaction width. So, widths for inelastic scattering and scattering with change of ℓ , $\ell' = \ell - 2$, were summed to form this width. The number of degrees of freedom for $\ell' = \ell - 2$ scat-

tering was applied because that width is always at least five times the inelastic scattering width. The only inelastic level below 100 kev is a $9/2^-$ level at 6.3 kev. No measured cross sections were found for it. The $\ell' = \ell - 2$ process occurs for (ℓ, J) states (2,3) and (2,4).

A listing of the energy dependent parameters for Ta^{181} is found in Table 7. These parameters may be used alternatively to the energy-independent parameters which were supplied for the ENDF/B file.

No fits were made for Ta^{182} because of the paucity of experimental data. Since only small concentrations of Ta^{182} are expected in reactors, energy-independent parameters were deemed adequate.

b. Energy-Independent Parameter Fit

The energy-independent parameter fit to the capture cross section data for Ta^{181} yielded the parameters shown in Table 8.

The fit is similar to the energy-dependent fit except for S_2 . The χ^2 value is 2.2 also, and the same comments with respect to the resolved resonance average parameters apply. The two fits plus their smooth cross sections will give the same infinitely dilute cross sections. Self-shielded cross sections will be slightly different.

For Ta^{182} , the observed $\langle D \rangle_{\ell=0}$ and $\langle \Gamma_\gamma \rangle$ are adopted. The strength functions are taken from the energy independent Ta^{181} fit. No smooth background is employed. Inelastic scattering is ignored. Levels exist at 16 and 97 kev.

c. ENDF/B File 3 Smooth Cross Section Data for Ta^{181}

Table 9 provides a tabulation of smooth background cross sections for both the energy-independent and energy-dependent fits. The smooth cross section when added to the cross section determined from resonance parameters will yield the evaluated cross sections listed in Table 4.

6. Comparison of Calculated and Measured Resonance Integrals

a. Ta^{181}

The capture resonance integral calculated from the evaluated resonance parameters plus smooth cross sections is 738.7 barns. This agrees well with a recent evaluation of measurements by Drake⁽³⁶⁾ which gave 740 ± 40 barns. A breakdown of the calculated result by component is given in Table 10.

TABLE 7
 LISTING OF ENERGY-DEPENDENT UNRESOLVED RESONANCE
 PARAMETERS FOR Ta¹⁸¹
 (Sheet 1 of 3)

| Energy, E (ev) | Angular Momentum, ℓ | Compound Nucleus Spin, J | Level Spacing, $\overline{D}_{\ell,J}$ (ev) | Competitive Reaction Width, $\Gamma_{x,\ell,J}$ (ev) | Reduced Neutron Width, $\Gamma_{n,\ell,J}^0$ (ev ^{1/2}) | |
|-------------------|-----------------------------|--------------------------------|--|---|--|-----------------------|
| 1.0×10^5 | 0 | 3 | 7.1643 | 3.34×10^{-2} | 1.11×10^{-3} | |
| | 0 | 4 | 6.3333 | 5.90×10^{-2} | 9.84×10^{-4} | |
| | 1 | 2 | 9.1119 | 8.13×10^{-4} | 6.57×10^{-4} | |
| | 1 | 3 | 7.1643 | 1.28×10^{-3} | 5.16×10^{-4} | |
| | 1 | 4 | 6.3333 | 3.02×10^{-1} | 4.56×10^{-4} | |
| | 1 | 5 | 6.0810 | 2.90×10^{-1} | 4.38×10^{-4} | |
| | 2 | 1 | 14.245 | 0.0 | 5.72×10^{-4} | |
| | 2 | 2 | 9.1119 | 0.0 | 3.66×10^{-4} | |
| | 2 | 3 | 7.1643 | 3.85×10^{-1} | 2.88×10^{-4} | |
| | 2 | 4 | 6.3333 | 3.70×10^{-1} | 2.55×10^{-4} | |
| | 2 | 5 | 6.0810 | 5.66×10^{-2} | 2.44×10^{-4} | |
| | 2 | 6 | 6.2347 | 5.81×10^{-2} | 2.51×10^{-4} | |
| | 5.0×10^4 | 0 | 3 | 7.7458 | 1.29×10^{-2} | 1.20×10^{-3} |
| | | 0 | 4 | 6.8511 | 2.29×10^{-2} | 1.06×10^{-3} |
| 1 | | 2 | 9.8473 | 1.37×10^{-4} | 7.10×10^{-4} | |
| 1 | | 3 | 7.7458 | 2.16×10^{-4} | 5.58×10^{-4} | |
| 1 | | 4 | 6.8511 | 2.23×10^{-1} | 4.94×10^{-4} | |
| 1 | | 5 | 6.5827 | 2.14×10^{-1} | 4.74×10^{-4} | |
| 2 | | 1 | 15.390 | 0.0 | 6.18×10^{-4} | |
| 2 | | 2 | 9.8473 | 0.0 | 3.96×10^{-4} | |
| 2 | | 3 | 7.7458 | 2.82×10^{-1} | 3.11×10^{-4} | |
| 2 | | 4 | 6.8511 | 2.61×10^{-1} | 2.75×10^{-4} | |
| 2 | | 5 | 6.5827 | 2.20×10^{-2} | 2.65×10^{-4} | |
| 2 | | 6 | 6.7547 | 2.26×10^{-2} | 2.71×10^{-4} | |

TABLE 7
 LISTING OF ENERGY-DEPENDENT UNRESOLVED RESONANCE
 PARAMETERS FOR Ta¹⁸¹
 (Sheet 2 of 3)

| Energy, E (ev) | Angular Momentum, ℓ | Compound Nucleus Spin, J | Level Spacing, $D_{\ell, J}$ (ev) | Competitive Reaction Width, $\Gamma_{x, \ell, J}$ (ev) | Reduced Neutron Width, Γ_n^0 (ev ^{1/2}) ^{ℓ, J} | |
|-------------------|-----------------------------|--------------------------------|--|---|---|-----------------------|
| 2.0×10^4 | 0 | 3 | 8.1181 | 2.58×10^{-3} | 1.26×10^{-3} | |
| | 0 | 4 | 7.1827 | 4.56×10^{-3} | 1.12×10^{-3} | |
| | 1 | 2 | 10.318 | 8.15×10^{-6} | 7.43×10^{-4} | |
| | 1 | 3 | 8.1181 | 1.28×10^{-5} | 5.85×10^{-4} | |
| | 1 | 4 | 7.1827 | 1.31×10^{-1} | 5.18×10^{-4} | |
| | 1 | 5 | 6.9042 | 1.26×10^{-1} | 4.97×10^{-4} | |
| | 2 | 1 | 16.123 | 0.0 | 6.48×10^{-4} | |
| | 2 | 2 | 10.318 | 0.0 | 4.15×10^{-4} | |
| | 2 | 3 | 8.1181 | 1.81×10^{-1} | 3.26×10^{-4} | |
| | 2 | 4 | 7.1827 | 1.62×10^{-1} | 2.89×10^{-4} | |
| | 2 | 5 | 6.9042 | 4.39×10^{-3} | 2.77×10^{-4} | |
| | 2 | 6 | 7.0882 | 4.50×10^{-3} | 2.85×10^{-4} | |
| | 1.0×10^4 | 0 | 3 | 8.2463 | 3.78×10^{-4} | 1.28×10^{-3} |
| | | 0 | 4 | 7.2970 | 6.69×10^{-4} | 1.13×10^{-3} |
| 1 | | 2 | 10.480 | 3.17×10^{-7} | 7.55×10^{-4} | |
| 1 | | 3 | 8.2463 | 4.99×10^{-7} | 5.94×10^{-4} | |
| 1 | | 4 | 7.2970 | 6.90×10^{-2} | 5.26×10^{-4} | |
| 1 | | 5 | 7.0151 | 6.63×10^{-2} | 5.05×10^{-4} | |
| 2 | | 1 | 16.376 | 0.0 | 6.58×10^{-4} | |
| 2 | | 2 | 10.480 | 0.0 | 4.21×10^{-4} | |
| 2 | | 3 | 8.2463 | 1.29×10^{-1} | 3.31×10^{-4} | |
| 2 | | 4 | 7.2970 | 1.14×10^{-1} | 2.93×10^{-4} | |
| 2 | | 5 | 7.0151 | 6.43×10^{-4} | 2.82×10^{-4} | |
| 2 | | 6 | 7.2032 | 6.60×10^{-4} | 2.89×10^{-4} | |

TABLE 7
 LISTING OF ENERGY-DEPENDENT UNRESOLVED RESONANCE
 PARAMETERS FOR Ta¹⁸¹
 (Sheet 3 of 3)

| Energy, E (ev) | Angular Momentum, ℓ | Compound Nucleus Spin, J | Level Spacing, $\bar{D}_{\ell,J}$ (ev) | Competitive Reaction Width, $\Gamma_{x\ell,J}$ (ev) | Reduced Neutron Width, $\Gamma_{n\ell,J}^0$ (ev ^{1/2}) |
|-------------------|-----------------------------|--------------------------------|---|--|---|
| 5.0×10^3 | 0 | 3 | 8.3112 | 0.0 | 1.29×10^{-3} |
| | 0 | 4 | 7.3549 | 0.0 | 1.14×10^{-3} |
| | 1 | 2 | 10.562 | 0.0 | 7.61×10^{-4} |
| | 1 | 3 | 8.3112 | 0.0 | 5.99×10^{-4} |
| | 1 | 4 | 7.3549 | 0.0 | 5.30×10^{-4} |
| | 1 | 5 | 7.0712 | 0.0 | 5.10×10^{-4} |
| 2.0×10^3 | 0 | 3 | 8.3112 | 0.0 | 1.29×10^{-3} |
| | 0 | 4 | 7.3898 | 0.0 | 1.15×10^{-3} |
| | 1 | 2 | 10.612 | 0.0 | 7.65×10^{-4} |
| | 1 | 3 | 8.3504 | 0.0 | 6.02×10^{-4} |
| | 1 | 4 | 7.3898 | 0.0 | 5.32×10^{-4} |
| | 1 | 5 | 7.1051 | 0.0 | 5.12×10^{-4} |
| 1.0×10^3 | 0 | 3 | 8.3635 | 0.0 | 1.30×10^{-3} |
| | 0 | 4 | 7.4015 | 0.0 | 1.15×10^{-3} |
| | 1 | 2 | 10.628 | 0.0 | 7.66×10^{-4} |
| | 1 | 3 | 8.3635 | 0.0 | 6.03×10^{-4} |
| | 1 | 4 | 7.4015 | 0.0 | 5.33×10^{-4} |
| | 1 | 5 | 7.1168 | 0.0 | 5.13×10^{-4} |
| 6.0×10^2 | 0 | 3 | 8.3688 | 0.0 | 1.30×10^{-3} |
| | 0 | 4 | 7.4061 | 0.0 | 1.15×10^{-3} |
| | 1 | 2 | 10.635 | 0.0 | 7.66×10^{-4} |
| | 1 | 3 | 8.3688 | 0.0 | 6.03×10^{-4} |
| | 1 | 4 | 7.4061 | 0.0 | 5.34×10^{-4} |
| | 1 | 5 | 7.1209 | 0.0 | 5.13×10^{-4} |
| 3.0×10^2 | 0 | 3 | 8.3727 | 0.0 | 1.30×10^{-3} |
| | 0 | 4 | 7.4097 | 0.0 | 1.15×10^{-3} |
| | 1 | 2 | 10.640 | 0.0 | 7.67×10^{-4} |
| | 1 | 3 | 8.3727 | 0.0 | 6.03×10^{-4} |
| | 1 | 4 | 7.4097 | 0.0 | 5.34×10^{-4} |
| | 1 | 5 | 7.1244 | 0.0 | 5.13×10^{-4} |

TABLE 8
 LISTING OF ENERGY-INDEPENDENT
 UNRESOLVED RESONANCE
 PARAMETERS FOR Ta¹⁸¹

| Parameter | Value | Uncertainty in Fit (%) |
|-----------------------------------|-------------------------|------------------------|
| $\langle D \rangle_{\ell=0}$ | 3,929 ev | 17 |
| $\langle \Gamma_{\gamma} \rangle$ | 64.0 mv | 31 |
| S ₀ | 1.60 x 10 ⁻⁴ | 40 |
| S ₁ | 0.49 x 10 ⁻⁴ | 120 |
| S ₂ | 0.0 x 10 ⁻⁴ | - |

TABLE 9
 FITTED SMOOTH BACKGROUND CROSS SECTIONS FOR Ta¹⁸¹

| Energy (kev) | Cross Sections for Energy-Independent Fit | | Cross Sections for Energy-Dependent Fit | |
|--------------|---|-----------------|---|-----------------|
| | Total (barns) | Capture (barns) | Total (barns) | Capture (barns) |
| 100 | +0.20 | -0.014 | +0.0006 | +0.0 |
| 50 | -0.29 | -0.010 | -0.396 | +0.0 |
| 20 | -0.96 | +0.037 | -0.955 | +0.023 |
| 10 | -1.58 | +0.055 | -1.489 | +0.020 |
| 5 | -2.97 | -0.113 | -2.740 | -0.177 |
| 2 | -4.95 | +0.006 | -4.588 | -0.017 |
| 1 | -6.61 | +0.661 | -6.07 | +0.69 |
| 0.6 | -5.21 | +1.00 | -4.50 | +1.09 |
| 0.3 | -8.40 | -1.90 | -7.38 | -1.68 |

TABLE 10
INFINITELY DILUTE RESONANCE INTEGRAL FOR
CAPTURE IN Ta¹⁸¹

| Description | Component of Integral (barns) |
|---|----------------------------------|
| Resolved Resonances (0.5 to 330 ev) | |
| Negative energy resonance | 1.37 |
| 4.28 ev resonance | 465.55 |
| Other 74 resonances | 243.52 |
| Unresolved Resonances (330 to 10 ⁵ ev) | |
| $l =$ resonances | 26.88 |
| $l = 1$ | 0.86 |
| $l = 2$ | 0.01 |
| Smooth Cross Section | 0.47 |
| Total | 738.66 |

About 63% of this resonance integral is contributed by the 4.28 ev resonance. Its level widths have quoted uncertainties of 5 to 8%, so such close agreement between the calculated and measured resonance integrals is fortuitous.

Effective capture self-shielding factors, $f = I_{\text{eff}}/I_{\infty}$, of tantalum foils were calculated with the TRIX code and compared to values calculated from the measurements of Pierce et al.⁽³⁷⁾ The overlap corrections of Pierce were included. The agreement was within experimental error over the entire range of foil thicknesses as shown in Table 11.

b. Ta¹⁸²

The capture resonance integral calculated from the evaluated resonance parameters is 1020 barns. A breakdown by component is given in Table 12. No measured values have been found in the open literature for comparison. The resonance integral of 943 ± 50 barns deduced by Stokes⁽³⁾ is in reasonable agreement with our value.

TABLE 11
COMPARISON OF SELF-SHIELDING FACTORS FOR Ta¹⁸¹

| (Surface/Mass) ^{1/2} | f _{measured} | f _{calculated} |
|-------------------------------|-----------------------|-------------------------|
| 82 | 0.952 ± 0.064 | 0.985 |
| 7.0 | 0.579 ± 0.035 | 0.555 |
| 3.13 | 0.322 ± 0.022 | 0.316 |
| 1.05 | 0.129 ± 0.006 | 0.132 |
| 0.50 | 0.0709 ± 0.0035 | 0.0735 |

TABLE 12
INFINITELY DILUTE RESONANCE INTEGRAL FOR
CAPTURE IN Ta¹⁸²

| Description | Component of Integral (barns) |
|--|----------------------------------|
| Resolved Resonances (0.5 to 35 ev) | |
| Negative energy resonance | 12.7 |
| 0.147 ev resonance | 715.2 |
| Other 8 resonances | 154.1 |
| Unresolved Resonances (35 to 10 ⁵ ev) | |
| l = 0 resonances | 137.0 |
| l = 1 | 0.8 |
| l = 2 | 0.0 |
| Total | 1019.8 |

III. EVALUATION OF CROSS SECTION DATA ABOVE 100 kev

A. THEORETICAL CALCULATIONS

1. Introduction

A complete set of neutron cross sections was calculated for each isotope in the energy range between 100 kev and 17 Mev. The calculations were carried out on an energy grid which was fine enough to provide an adequate shape description of the various reaction cross sections. A deformed optical model was used to describe the total cross section and all direct processes. A statistical model of the compound nucleus was used to separate the compound nucleus formation cross section into its constituent parts.

2. Optical Model Calculations

The optical model has been used successfully to describe a part of the interaction between nucleus and nuclei. It has been shown that a deformed nucleus potential such as in the 2-PLUS code should be used to describe the interaction of neutrons with even-even tungsten isotopes.⁽³⁸⁾ As tantalum has a deformed nucleus, but is not even-even, the more general case solved by the JUPITOR code was investigated.⁽³⁹⁾ The use of JUPITOR was abandoned because of excessive running time and other problems. The more restricted even-even nucleus model offered by 2-PLUS⁽⁴⁰⁾ was adopted. A brief investigation of this approximation assured us that no greater model uncertainty would be introduced.

Comparison of calculation with available experimental data in the form of total cross sections, elastic angular distributions, and neutron strength functions demonstrated that the parameters previously recommended for the even tungsten isotopes were still the optimum parameters.⁽⁴¹⁾ This set of parameters is given in Table 13 and they were used for all isotopes analyzed. The difference between results of calculations for the different isotopes was negligible. An average deformation ($\beta = 0.21$) was assumed and only the first excited level in the ground state rotational band was strongly coupled in the calculational model.

The optical model calculations supplied the following quantities:

- 1) Total cross section
- 2) Direct elastic scattering

TABLE 13
DEFORMED NUCLEUS OPTICAL MODEL PARAMETERS

| | |
|---|-----------------------------|
| Real Saxon Well Depth | 45.05 - 0.3E Mev |
| Real Saxon Well Radius | 1.25 A ^{1/3} Fermi |
| Real Saxon Well Diffuseness | 0.65 Fermi |
| Imaginary Saxon Derivative Well Depth | 6.68 + 1.3√E Mev |
| Imaginary Saxon Derivative Well Radius | 1.25 A ^{1/3} Fermi |
| Imaginary Saxon Derivative Well Diffuseness | 0.47 Fermi |
| Spin Orbit Well Depth | 6.2 Mev |
| Deformation Parameter | 0.21 |

- 3) Direct inelastic scattering
- 4) Legendre moments for 2 and 3
- 5) Transmission coefficients for compound nucleus formation

Only the total cross section can be used directly in an evaluation at all neutron energies. The scattering cross sections and their Legendre components may have additional contributions from compound nucleus reactions. Therefore, the compound nucleus decay must be analyzed in a manner consistent with the optical model calculations. In fact, all parameters listed above and obtained from optical model calculations are supplied as input to the statistical compound nucleus theory calculations.

3. Statistical Compound Nucleus Calculation

A comprehensive model of compound nucleus calculations has been described recently.⁽⁴²⁾ The details have been incorporated in a computer program, COMNUC, which was used to provide the reaction channel components of the reaction cross section. The program has been designed to take the output from an optical model calculation, combine it with the compound nucleus calculation, and provide as output a complete and mutually consistent set of cross sections at selected incident neutron energies.

In contrast to the optical model calculations, the statistical theory calculations were performed for each isotope since the statistical model parameters differed greatly between isotopes. A gamma ray cascade calculation⁽⁴²⁾ was

carried out for each isotope up to an energy of 4 Mev. The results of this calculation were used as input to the compound nucleus calculation and permitted a more accurate calculation of the capture cross section in the region of transition between neutron energies where the capture cross section is the gamma emission cross section and neutron energies where capture occurs only when gamma ray energies exceed the neutron binding energy.

A compound nucleus calculation is performed by calculating the contribution to each outgoing reaction channel from each compound nucleus state (J, angular momentum; and π , parity). The formation of these compound nucleus states is determined by the transmission coefficients from the deformed nucleus optical model and spin and parity conservation. Each outgoing channel reaction type and its model parameters will be described in succeeding paragraphs.

Neutron capture cross sections were calculated using a single particle dipole emission model. This model is discussed by Blatt and Weisskopf.⁽⁴³⁾ The model incorporates the nuclear level density formula of Cook et al.⁽¹³⁾ The last neutron binding energy, E_b , and the gamma ray strength function $\langle 2\pi\Gamma_\gamma/D \rangle$ from measured low energy s-wave resonances are required input. The value, E_b , was obtained from Wapstra's latest mass tables.⁽⁴⁴⁾ The gamma ray strength function obtained from resolved resonance parameters for Ta¹⁸¹ did not lead to capture cross sections consistent with available measured values. The parameter was adjusted by a factor (0.758) to match available data at 100 kev. The Ta¹⁸² experimental strength function was multiplied by the same scale factor. These data are summarized in Table 14.

The level structure adopted for each isotope is given in Table 15. For odd Z or odd A isotopes the level bands based on isomeric states were excluded because experimental excitation of these levels has not been observed in neutron scattering experiments. They are seen only in γ -ray decay, β -decay, and other similar processes. Continuum inelastic cross sections were calculated for energies above the last resolved discrete level. Channel probabilities were obtained by integration of energy-dependent spherical transmission coefficients over an analytic expression for the level density.⁽¹³⁾

At all energies where there are less than 40 open channels, the correlation correction factor is calculated and applied.⁽⁴²⁾ In all cases Moldauer's Q factor (References 45 and 46) has been set to 0. Compound nucleus angular distribution

Legendre moments are calculated and merged with the direct components when necessary.

B. EVALUATED DATA

1. Radiative Capture Cross Sections

Above 100 keV smooth cross sections were specified for the tantalum isotopes in ENDF/B File 3. In the case of Ta^{182} , these data were derived entirely from theory. Arguments for the choice of capture cross section in the neighborhood of 100 keV were presented in Section II-B. From 100 to 140 keV a visual fit was made from the data of Kompe,⁽²²⁾ Brzosko,⁽²³⁾ and Miskel.⁽²⁶⁾ The capture

TABLE 14
CAPTURE MODEL PARAMETERS FOR TANTALUM

| | B.E. (MeV) | $\langle 2\pi\Gamma_{\gamma}/D \rangle$ |
|------------|---------------|---|
| Ta^{181} | 5.92 | 0.06065 |
| Ta^{182} | 6.85 | 0.09116 |

TABLE 15
LEVEL DIAGRAMS FOR TANTALUM ISOTOPES

| Ta^{181} | | Ta^{182} | |
|-----------------|-------------|-----------------|-------------|
| Energy (MeV) | Spin-Parity | Energy (MeV) | Spin-Parity |
| 0.0 | $7/2^+$ | 0.0 | 3^- |
| 0.136 | $9/2^+$ | 0.097 | 4^- |
| 0.302 | $11/2^+$ | 0.114 | 4^- |
| 0.482 | $5/2^+$ | 0.173 | 5^- |
| 0.499 | $13/2^+$ | 0.237 | 5^- |
| 0.615 | $1/2^+$ | 0.270 | 2^- |
| 0.619 | $5/2^+$ | 0.292 | 5^- |
| 0.699 | $3/2^+$ | 0.315 | 6^- |
| 0.797 | $9/2^+$ | 0.360 | 3^- |
| 0.838 | $5/2^+$ | 0.400 | Continuum |
| 1.00 | Continuum | | |

data of Fricke⁽¹⁹⁾ tend to remain high in this energy range. Upon renormalization, the data of Macklin and Gibbons,^(21,27) and Kononov⁽²⁹⁾ support the evaluation made in this energy range. From 140 to about 240 keV the numerous experiments were found to be in good agreement. From 240 keV up to 2 MeV we relied upon the data of Fricke,⁽¹⁹⁾ Brzosko,⁽²³⁾ and Cox⁽⁴⁷⁾ which were in close agreement. Limited guidance was provided by the somewhat oscillatory data of Miskel⁽²⁶⁾ in this energy range.

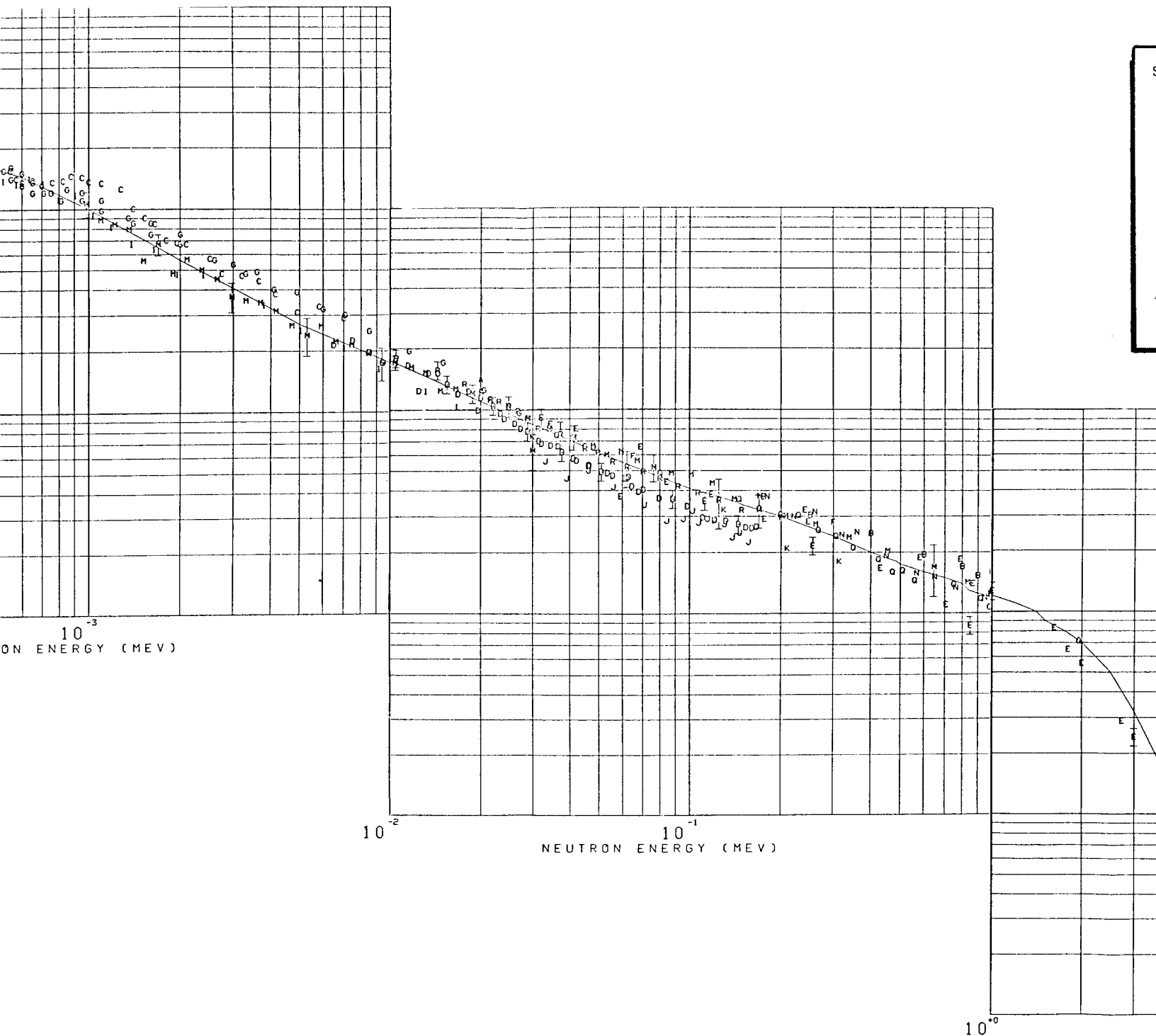
Above 2 MeV, considerable uncertainty exists regarding the capture cross section, as it rapidly approaches zero. In this region, the data of Miskel were used in preference to those of Kompe⁽²²⁾ as the former agree better with the shape of our theoretical calculations.

Above 5 MeV, no data exist for the capture cross section. The theory of Benzi and Reffo⁽⁴⁸⁾ was utilized to describe the collective and direct interaction capture cross sections to 17 MeV. For these calculations, the nuclear deformation, β , was taken to be 0.265 for both isotopes. The nuclear radius, R , was taken to be $1.2 A^{1/3}$ fermis. Credibility of these calculations is reasonable based upon agreement with the measurement available in the neighboring nucleus, W^{186} , at 14.5 MeV.⁽⁴⁹⁾ The Ta^{181} capture cross section curve with data references is shown in Figure 4.

2. Total Cross Section

Total cross sections were specified for the tantalum isotopes in ENDF/B File 3. Again, in the case of Ta^{182} , these data were derived entirely from the results of the 2-PLUS and COMNUC computer runs.

The total cross section for Ta^{181} just above 100 keV was established from the 1949 University of Wisconsin measurements of Bockelman⁽³⁰⁾ and the time-of-flight data of A. B. Smith.^(50,51) Bockelman's measurements were done at 0° and at 115° . Above 250 keV, the measurements at 115° deviated markedly from those at 0° and were ignored. Data were received from Divadeenam⁽⁵²⁾ at Duke University (1970) which revised the 1965 Duke measurements in the energy range above 100 keV (see Table 5). Smith's data and the newer Duke measurements agree quite well up to their maximum energies of 650 keV. From 700 keV to 1 MeV, the 1967 RPI measurements of Martin^(53,54) were relied upon.



N

Both Smith and Martin's data contain considerable fluctuations which were arithmetically averaged. Together with the 1970 Duke measurements they provide a relatively smooth curve with minimal error band for the region from 100 keV to 1 MeV. In comparison the 2-PLUS calculated cross sections were generally about 0.1 barn below these experimental results. The energy variations agreed well. Above 1 MeV there are quite a few sets of experimental data (shown in Table 16) which were evaluated for this study. Several of these sets were also arithmetically averaged to smooth out fluctuations. The resulting curve and error band from these data extend from 1 through 15.6 MeV.

TABLE 16
SELECTED REFERENCE DATA FOR Ta¹⁸¹ TOTAL CROSS SECTION
MEASUREMENTS ABOVE 1 MeV

| Author | Laboratory | Year | Energy Range (MeV) | Source of Neutrons | Reference |
|-------------------------------------|----------------------------------|------|--------------------|-----------------------|-----------|
| R. C. Martin | Rensselaer Polytechnic Institute | 1967 | 0.6 to 25 | Li ⁷ (p,n) | 53,54 |
| D. W. Miller et al | University of Wisconsin | 1952 | 0.05 to 3.2 | T(p,n) | 56 |
| N. Neresen and S. Darden | Los Alamos | 1954 | 3.0 to 12 | Reactor | 57 |
| D. G. Foster, Jr. and D. W. Glasgow | Pacific NW | 1967 | 2.5 to 15 | Li ⁷ (d,n) | 58 |
| A. Bratenahlet al | Livermore | 1958 | 7.0 to 14 | D(d,n) | 59 |
| J. P. Conner | Los Alamos | 1958 | 13.1 to 15.6 | T(d,n) | 60 |

The 2-PLUS theoretical curve fell below the error band by amounts varying from 0.0 to 0.3 barn. The disagreement was greatest in the energy range 2.5 to 7 MeV. In this range theoretical calculations by Holmqvist and Wielding⁽⁵⁵⁾ agree much closer with our experimental evaluation. That work was performed with a 5-parameter ABACUS II search routine minimizing the difference in angular scattering measurements.

In summary, however, we find that the 2-PLUS calculations with slight adjustments adequately represent the Ta¹⁸¹ total cross section over the fast energy range. This is important as it tends to validate the use of adjusted 2-PLUS calculations for other reactions. Figure 5 shows the adopted total cross section curve for Ta¹⁸¹.

3. Elastic Cross Sections and Angular Distributions of Elastically Scattered Neutrons

The elastic data is specified in ENDF/B File 3, while the angular distributions are specified in File 4. Theory was used for the Ta¹⁸² file.

Little experimental data are available for the Ta¹⁸¹ elastic cross section. Below 100 kev there apparently is none available. Above 100 kev there are essentially two large sets of data and six single-energy experiments, the references for which, may be found in CINDA.

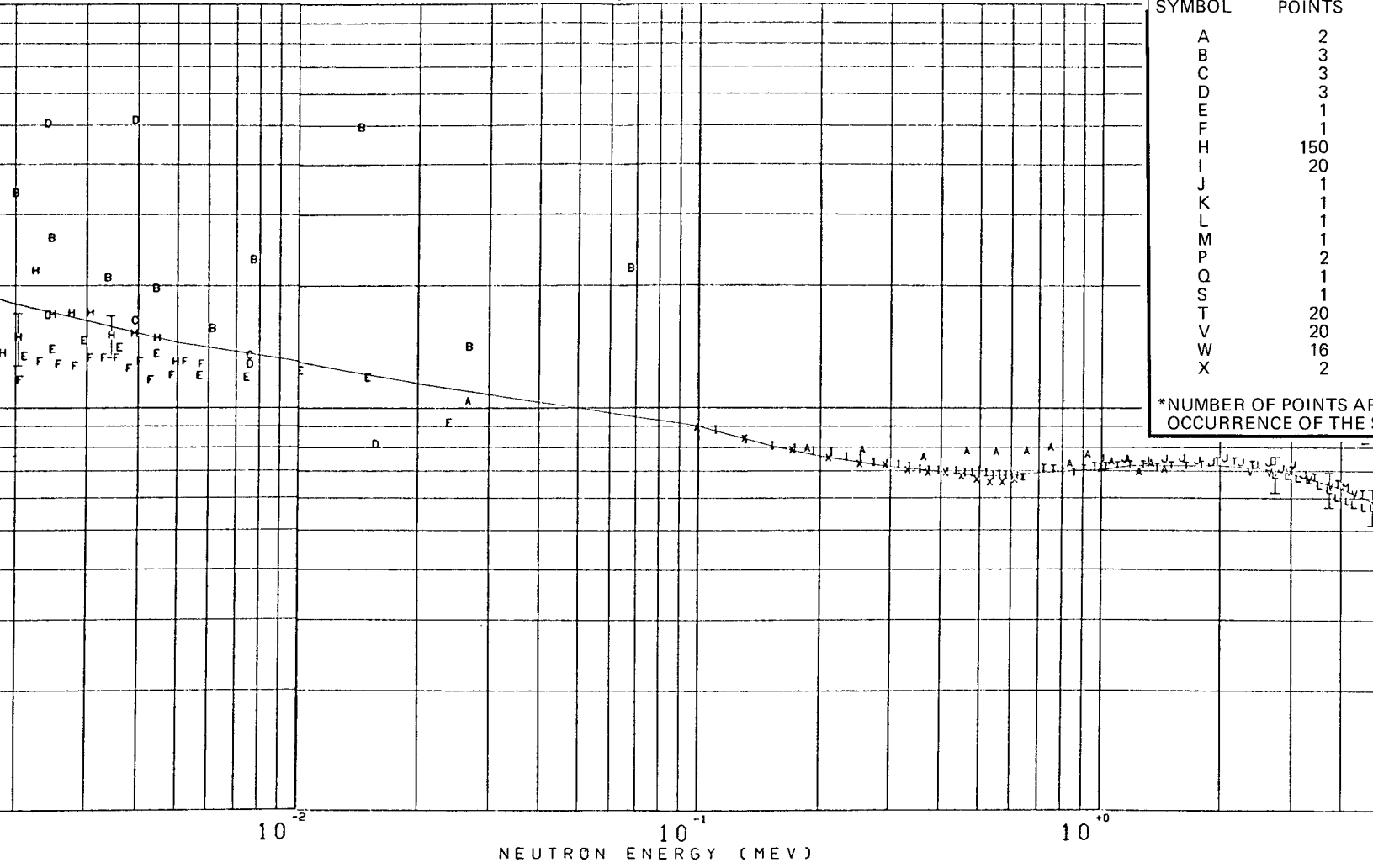
The two large sets of data are those of Smith⁽⁵¹⁾ and Holmqvist.⁽⁵⁵⁾ The theoretical cross sections generated in this study consisted of shape elastic scattering obtained from 2-PLUS and compound elastic scattering obtained from the COMNUC code. Comparison of these calculations to Holmqvist's data and to most of the single-energy experimental points show good agreement.

Comparison to the experimental points of Smith shows relatively poor agreement. Two observations regarding the Smith data must be noted, however. First Smith measured total, elastic, and inelastic cross sections. The sum of the elastic and inelastic measurements is considerably greater than the total measurement. This occurs over most of the range measured (300 kev to 1.5 Mev). Secondly, the sum of our calculated elastic cross section plus the partial cross section exciting the 136 kev level gives excellent agreement with Smith's quoted elastic cross section. This suggests that Smith was unable to completely resolve the 136 kev excitation from the elastic cross section. Indeed they show only a single data curve for the doublet centered at 144 kev, and indicate that the excitation of the lower energy state of the pair was roughly 1.6 times more intense than that of the higher energy state.

The Ta¹⁸¹ theoretical calculations of the elastic cross section were adopted with the following changes: small increases were made in the elastic cross section corresponding to adjustments made in the total cross section, and minor changes were also made to the elastic cross section corresponding to differences between the evaluated radiative capture cross section and COMNUC results above 100 kev.

These modifications produce an evaluated elastic cross section which is in good agreement with those of Holmqvist and most of the single-energy-point experimental data.

TA-181 TOTAL REACTION



| SYMBOL | POINTS** |
|--------|----------|
| A | 2 |
| B | 3 |
| C | 3 |
| D | 3 |
| E | 1 |
| F | 1 |
| H | 150 |
| I | 20 |
| J | 1 |
| K | 1 |
| L | 1 |
| M | 1 |
| P | 2 |
| Q | 1 |
| S | 1 |
| T | 20 |
| V | 20 |
| W | 16 |
| X | 2 |

*NUMBER OF POINTS AP
 OCCURRENCE OF THE

Theoretical values of the angular distribution of elastically scattered neutrons for the tantalum isotopes were obtained from the 2-PLUS and COMNUC calculations. Legendre coefficient data was printed out directly. The derived quantities, $\bar{\mu}_{lab}$, ξ , and γ were calculated from the angular distributions using the CHAD code.⁽⁶¹⁾

Plots of the Ta¹⁸¹ calculated elastic angular distributions compare favorably with Smith,⁽⁵¹⁾ Walt,⁽⁶²⁾ and Rogers⁽⁶³⁾ below 1 Mev. Figure 6 shows a typical plot at lower neutron energies. Above 1 Mev, a wide selection of experiments referenced in CINDA were used to compare to the theoretical distributions. Agreement was found to be good at the forward-scattering angles which is all elastic. The disagreements at other angles are attributed to inclusion of inelastic neutrons in the measured angular distributions. Figure 7 is a typical comparison.

The angular distributions were assumed isotropic in the center-of-mass system from thermal energies to 10 kev. Linear interpolation of the Legendre coefficients was assumed between 10 and 100 kev.

4. Inelastic Cross Section and Angular Distributions of Inelastically Scattered Neutrons

No experimental data were available for the evaluation of Ta¹⁸². A few sets of experimental data were available for evaluation of the Ta¹⁸¹ partial excitation functions. The most extensive were those of Smith⁽⁵¹⁾ and the MIT measurements of Rogers et al.⁽⁶⁴⁾ None of the available data was adequate to define a suitable set of partial inelastic excitation functions. Consequently, comparison of theory and measurement was of limited value. In general, where comparison was possible, the agreement was reasonable. This generally meant adding up the theoretical excitation functions for several levels to compare to one "experimental average" excitation function. Figure 8 shows comparisons with the COMNUC results.

Comparison was made, however, between calculation and the measured Ta¹⁸¹ total inelastic cross section. Summed partial excitation data to 1.5 Mev showed reasonable agreement within the band of fluctuations. Above 5 Mev, the data of Owens,⁽⁶⁵⁾ Rosen,⁽⁶⁶⁾ and Thomson,⁽⁶⁷⁾ substantiate the theoretical calculations which formed a basis for the evaluated cross sections.

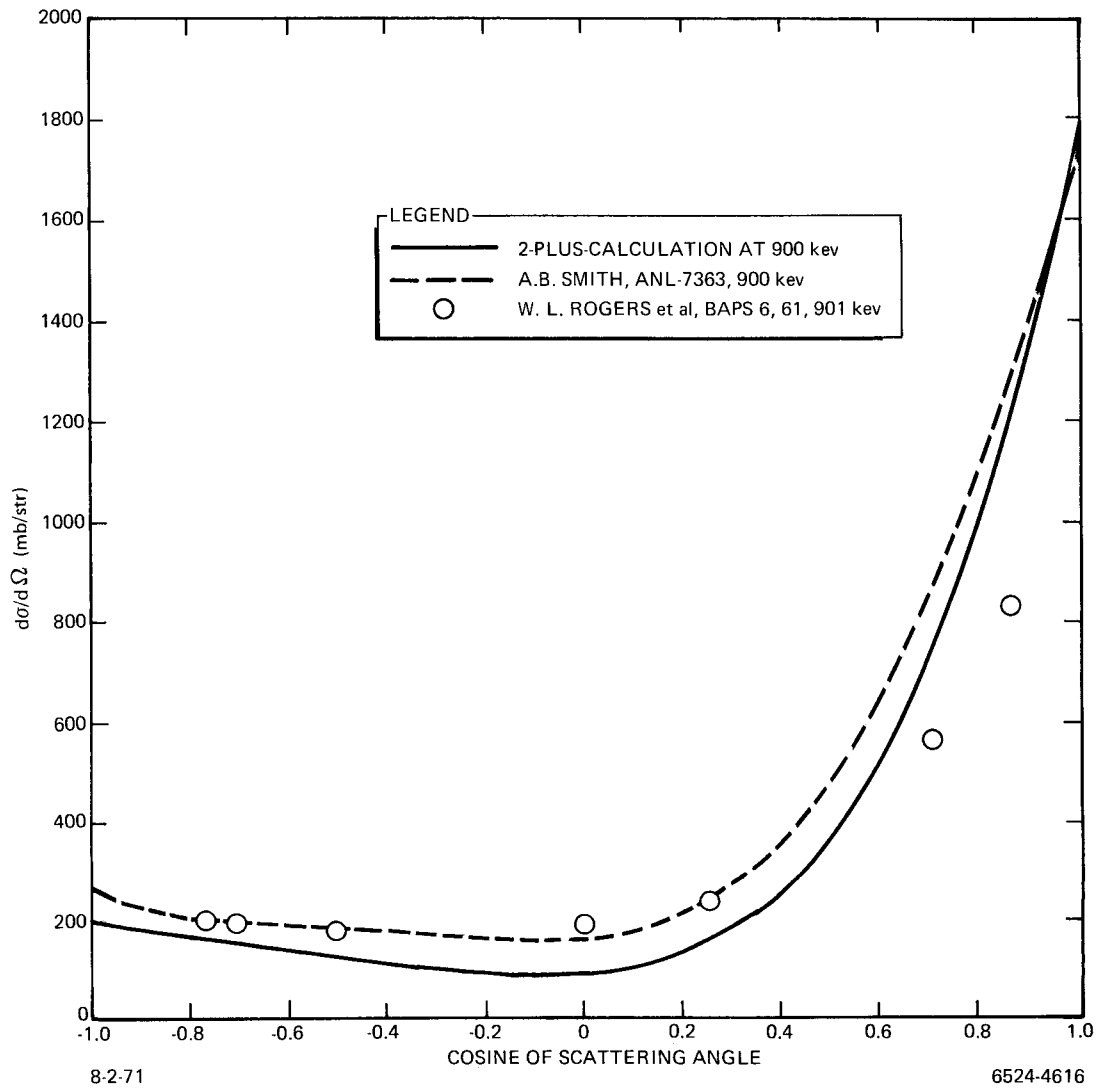


Figure 6. Ta^{181} Differential Elastic Scattering Cross Section (900 to 901 keV)

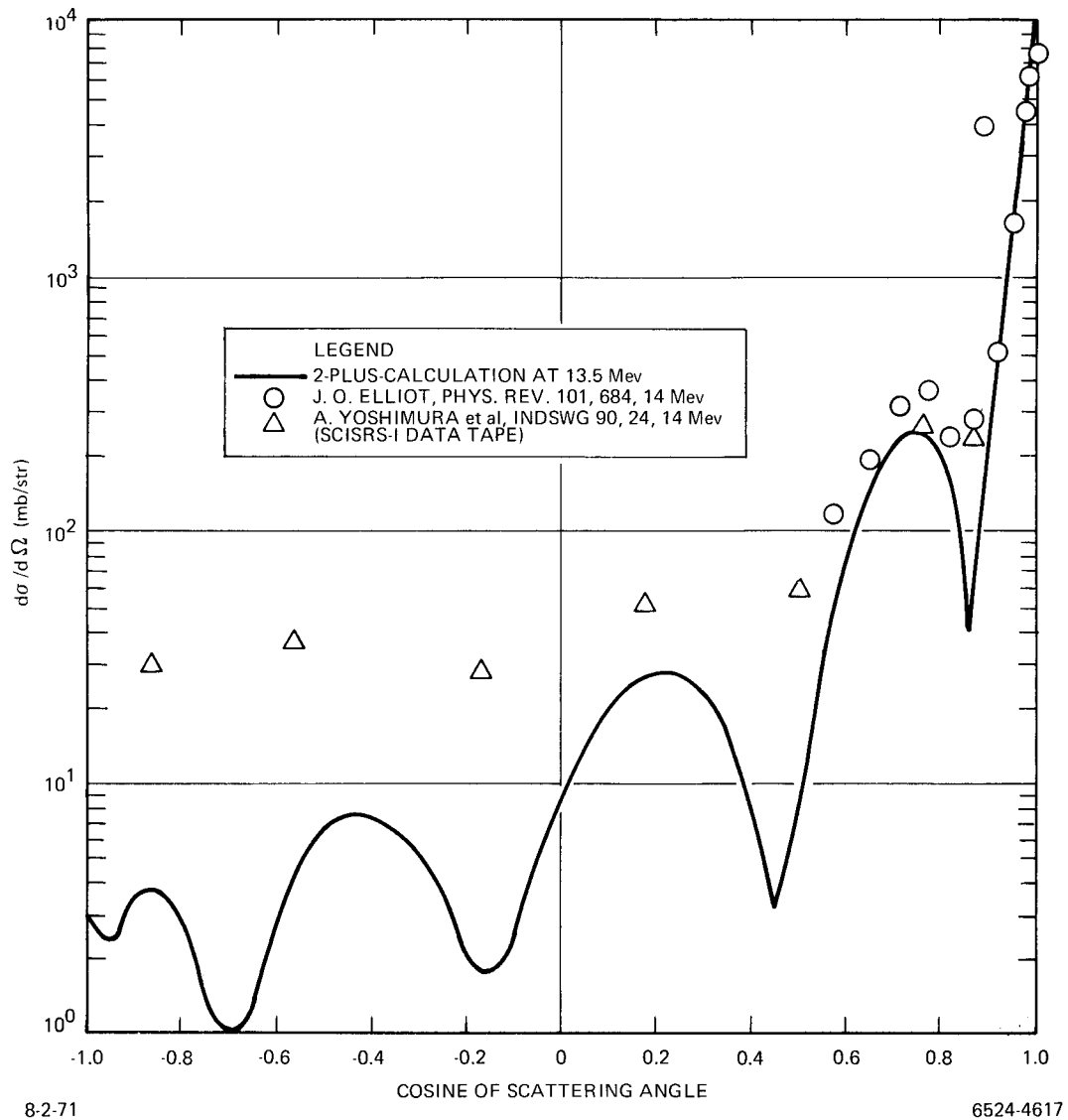
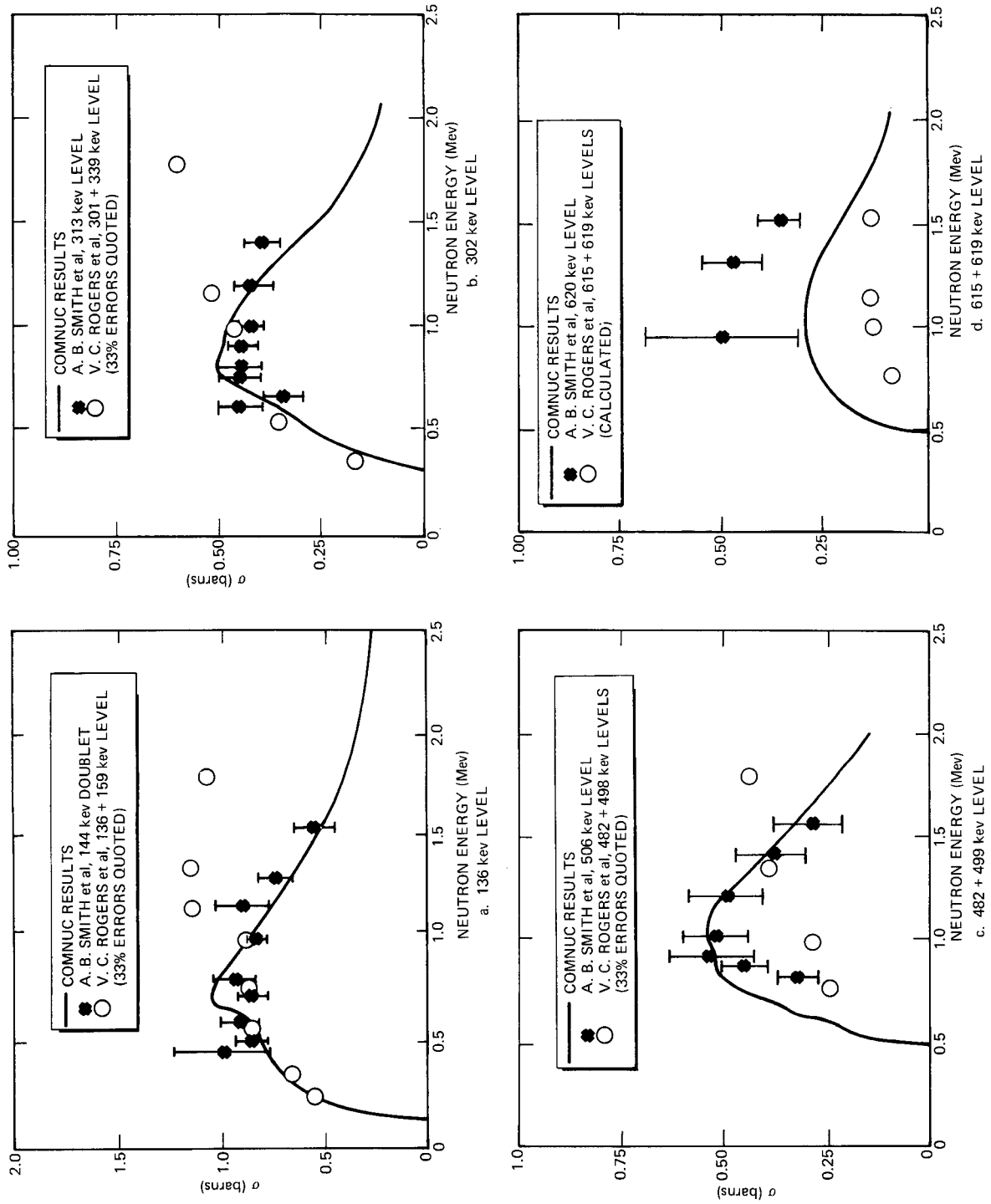


Figure 7. Ta^{181} Differential Elastic Scattering Cross Section (13.4 to 14.0 Mev)



6524-4618

8-2-71

Figure 8. Inelastic Excitation of Ta¹⁸¹

In the case of Ta^{182} the cross sections for exciting individual levels calculated with COMNUC were adopted, with minor changes at energies near the threshold of 0.0975 Mev. Structure in the 97-kev level cross sections calculated by COMNUC near the threshold was smoothed out. Similar structure calculated for the 2nd level (114 kev) was also smoothed out near threshold. The smoothing procedure was constrained by the total inelastic cross section. The structure was believed to be caused by competition for open channels due to the fact that the 1st level is weakly coupled and the 2nd level strongly coupled to the ground state.

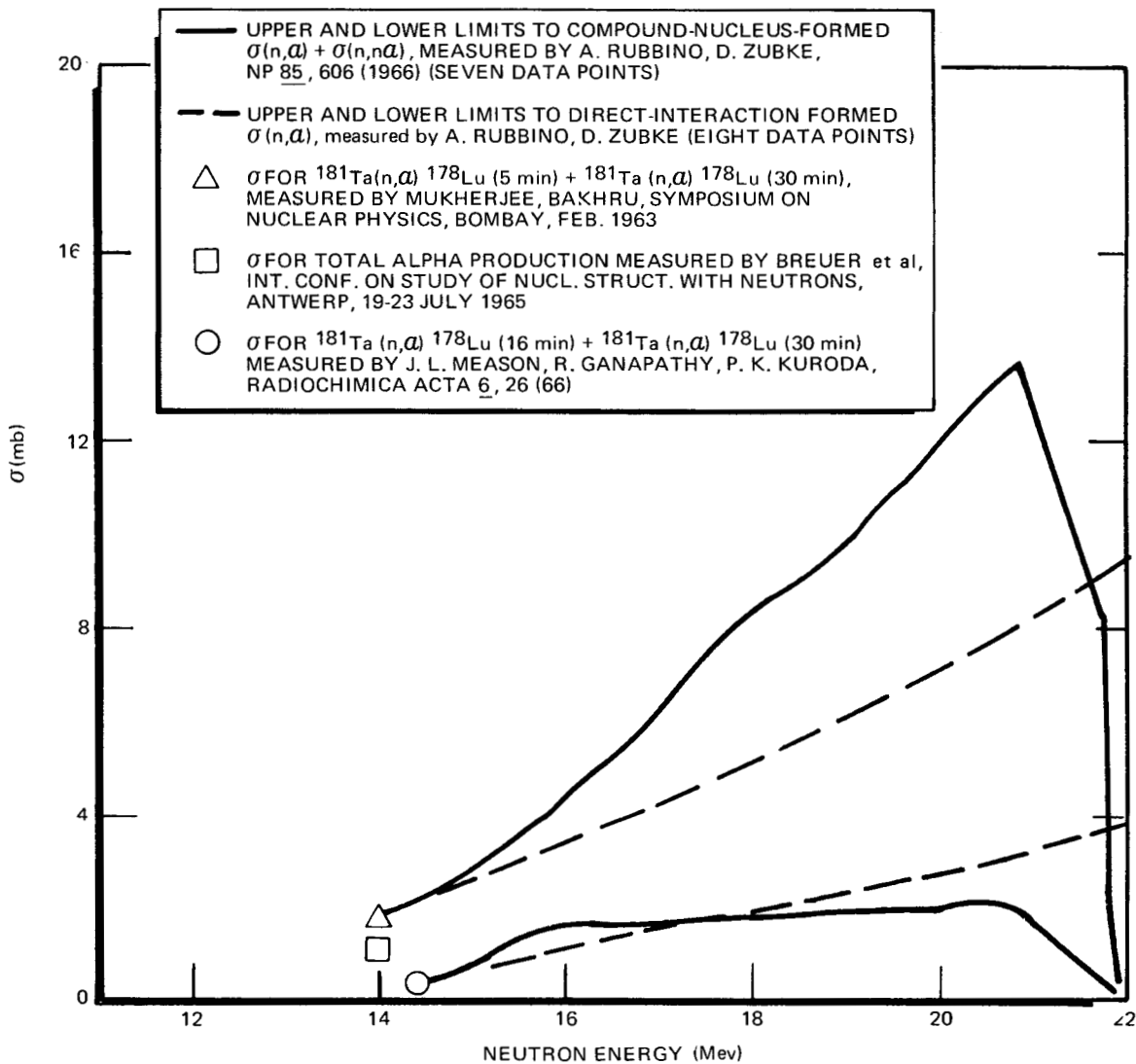
Below 3 Mev, the theoretical calculations included 9 levels (Ta^{181}) or 8 levels (Ta^{182}) plus a continuum. The continuum represents both the $(n,\gamma n)$ process and the $(n,n\gamma)$ excitation above the 9th (or 8th) level. The $(n,\gamma n)$ process involves a photon cascade and could not be allocated to a specific energy level.

Discrete level angular distributions were specified in ENDF/B File 4. Very limited experimental data exist for differential inelastic scattering. The little data observed offer no opposition to the decision to make all level distributions isotropic in the center-of-mass frame for both isotopes. The continuum was made isotropic in the lab frame.

5. Cross Sections for the $(n,2n)$ and $(n,3n)$ Reaction

The thresholds for the $(n,2n)$ and $(n,3n)$ reaction were obtained from Mat-
tauch et al.⁽⁴⁴⁾ For Ta^{181} , the thresholds are at 7.68 and 14.49 Mev, respectively. The Ta^{182} thresholds are lower; at 6.10 and 13.79 Mev, respectively. The only experimental data available were for the $Ta^{181}(n,2n)Ta^{180}$ reaction. These are referenced in CINDA.

Most of the experimental measurements appear to be on the high energy side of the peak $(n,2n)$ excitation. Some of the $(n,2n)$ experiments measured only cross section energy dependence. Of the experiments reporting absolute cross sections, four measured electron decay from Ta^{180} . Considerable discrepancy was resolved by renormalizing three of these experiments, which used a 1951 electron yield estimate,⁽⁶⁸⁾ to a 1962 electron yield estimate.⁽⁶⁹⁾ The electron counting experiments were then found to be in much better agreement with experiments measuring prompt neutrons and decay photons. The only serious disagreement was with the single and high valued 14-Mev data points of Ashby⁽⁷⁰⁾ ($2.64 \pm$



8-2-71

6524-4619

Figure 9. $\text{Ta}^{181}(n,\alpha)$ and $\text{Ta}^{181}(n,n\alpha)$ Measurements

0.2b) and Poularikas⁽⁷¹⁾ ($2.74 \pm 0.03b$). No details were given in the article by Poularikas et al⁽⁷¹⁾ except that the measurement was for the isomeric Ta^{181} ($n,2n$) Ta^{180m} (8 hour) reaction. Study of the article by Ashby et al⁽⁷⁰⁾ indicates that a large number of corrections were made to the original data. Both measurements were disregarded in this study. A consistent curve was constructed from the remaining data which lies higher than the previous ENDF/B evaluated curve.⁽⁷²⁾ Our new curve is slightly lower than that predicted theoretically by Pearlstein.⁽⁷³⁾ This agrees with comparisons of other isotopes to Pearlstein's predictions. For Ta^{182} , the adopted cross section data set was obtained by shifting the Ta^{181} curve to the Ta^{182} threshold.

Since no experimental data were available for the ($n,3n$) reaction, the adopted cross sections for both isotopes were obtained by simply subtracting the ($n,2n$) and inelastic continuum from the remaining nonelastic cross sections.

6. Cross Sections for the (n,α) Reaction

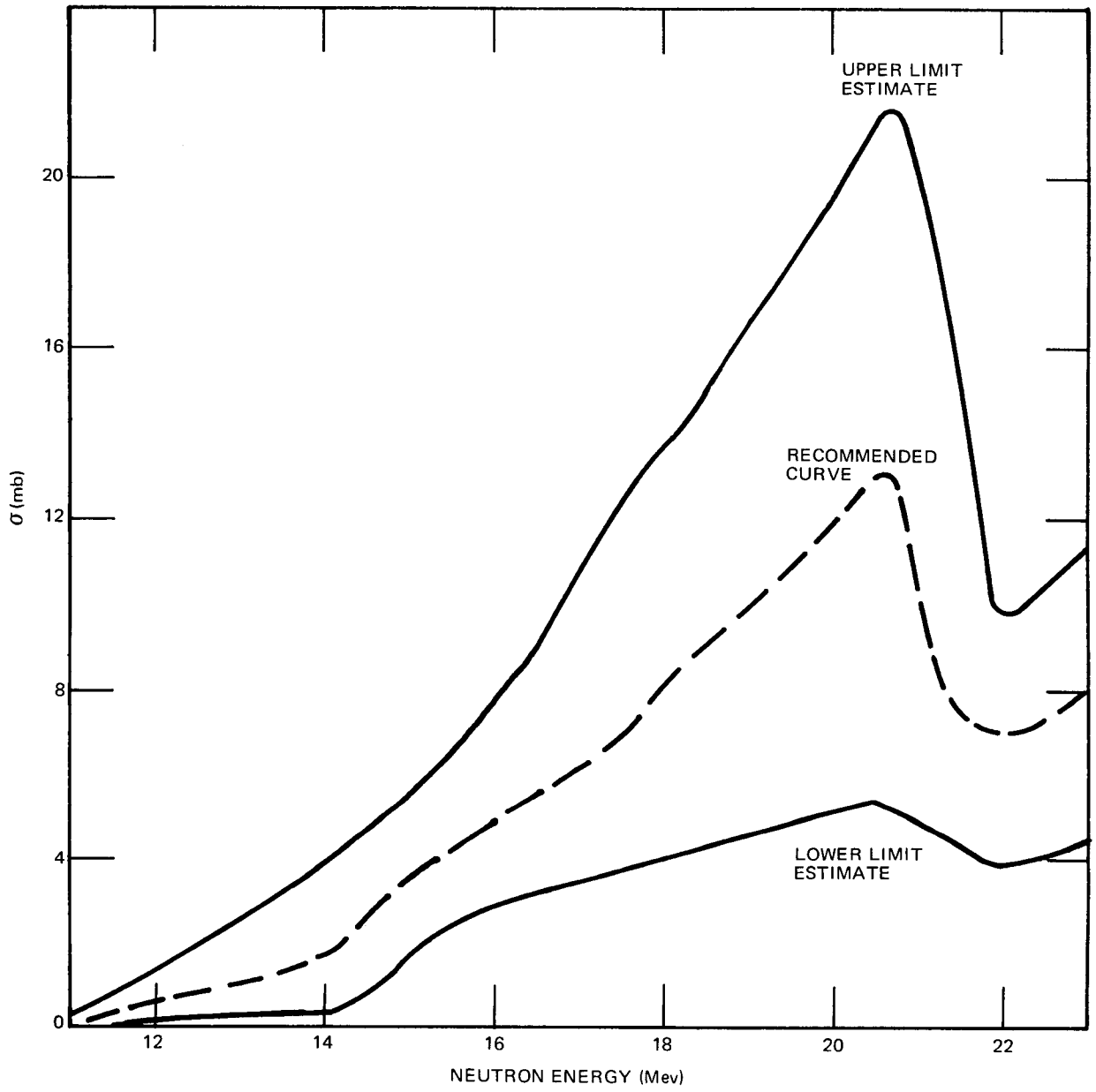
Figure 9 tabulates the Ta^{181} measurements for this reaction. The main contribution to our knowledge of this cross section is from the measurements of Rubbino and Zubke.⁽⁷⁴⁾ To obtain the cross section set for ENDF/B, the compound nucleus reactions and the direct interaction measurements were added to form the total (n,α) + ($n,n\alpha$) cross section. Figure 10 shows the results of adding the respective experimental data and limits, and evaluating a recommended cross section curve. The same cross sections were used for the Ta^{182} file.

7. Cross Sections for the (n,p) Reaction

The (n,p) cross section, being small and not well known, was not put in the ENDF/B data file. Figure 11 shows a recommended curve for the Ta^{181} (n,p) Hf^{181} reaction based upon measurements of the intensity of the $E_\gamma = 482$ keV line accompanying the decay of Hf^{181} . The (n,np) cross section, with a higher threshold energy, must also be considered. The dotted line in Figure 12 shows the evaluated (n,p) curve of Henderson⁽⁷²⁾ for ENDF/B material 1035.

8. Secondary Neutron Energy Distributions

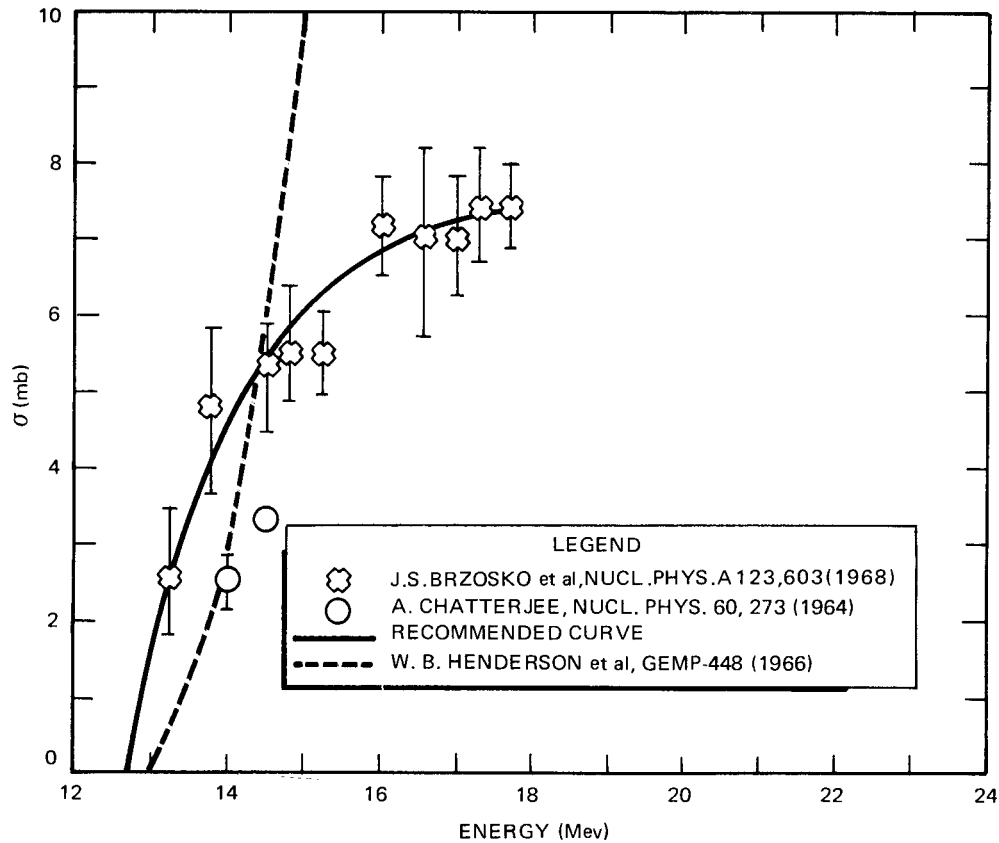
The ENDF/B File 5 contains data for the energy distributions of secondary neutrons. These distributions are expressed as normalized probability distributions,



8-2-71

6524-4620

Figure 10. Evaluated Cross Sections for the $Ta^{181} (n, \alpha) + Ta^{181} (n, n\alpha)$ Reaction



8-2-71

6524-4621

Figure 11. The $\text{Ta}^{181}(n,p)\text{Hf}^{181}$ Reaction

$$P(E \rightarrow E') = \sum_{k=1}^{NK} P_k(E) f_k(E \rightarrow E') \quad ,$$

where $P_k(E)$ is the fractional probability that the distribution $f_k(E \rightarrow E')$ is used at incident energy, E .

The partial energy distribution for tantalum has been specified by a Maxwellian evaporation spectrum

$$f(E \rightarrow E') = \frac{E'}{I} e^{-E'/\theta} \quad .$$

I is the normalization constant and θ is the incident energy dependent nuclear temperature.

Data presented by Owens and Towle,⁽⁶⁵⁾ Tsukada et al,⁽⁷⁵⁾ and Buccino et al⁽⁷⁶⁾ indicate that the nuclear temperatures can be expressed adequately as a function of excitation energy, E^* , by the expression:⁽⁷⁷⁾

$$\theta(E) = \left(\frac{E^*}{a} \right)^{1/2}$$

where

$$E^* = E_{\text{inc}} - E_{\text{th}}$$

E_{inc} = incident neutron energy

E_{th} = threshold energy for the inelastic process

$$= 137 \text{ kev for Ta}^{181}.$$

This formulation was used for the continuum inelastic neutrons. The level density parameter, a , was evaluated from the reference data. The value $a = 17.4$ fits Ta^{181} adequately over most of the continuum energy range and was used for Ta^{182} .

For the (n,2n) reaction the energy distribution of the emitted neutrons was specified by a mixture of Maxwellian evaporation spectra. Here $P_1(E) = P_2(E) = 1/2$ for all incident neutron energies. The characteristic nuclear temperature of the first emitted neutron, θ_1 , was assumed to be the same as that prescribed for the inelastic continuum process above. θ_2 was approximated from above with $E_2^* = E - 2\theta_1 - E_b$. Here E_2^* is the excitation energy of the residual nucleus following emission of the second neutron, $2\theta_1$ is the average kinetic energy of the first emitted neutron, and E_b is the binding energy of the second emitted neutron (7.68 Mev for Ta^{181} , 6.10 Mev for Ta^{182}).

The approximation is not valid for energies $-2\theta < E^* < 0$. Here the nuclear temperatures were held at a constant value, somewhat lower than the calculated in the transition energy range.

A similar evaluation was used for the (n,3n) reaction. θ_3 was evaluated with $P_k(E) = 1/3$ and the excitation energy, $E_3^* = E - E_b - 2\theta_1 - 2\theta_2$. For this reaction, $E_b = 14.49$ Mev for Ta^{181} and 13.79 Mev for Ta^{182} .

REFERENCES

1. M. D. Goldberg, S. F. Mughabghab, S. N. Purohit, B. A. Magurno, and V. M. May, BNL-325, 2nd Ed., Suppl. No. 2, IIC (1966)
2. O. A. Wasson, Nucl. Phys., A132, p 161 (1969)
3. G. E. Stokes, R. P. Schuman, and O. D. Simpson, Nucl. Sci. Eng., 33, p 16 (1968)
4. K. K. Seth, "Nuclear Size by Potential-Scattering Cross Sections," ORNL-2309, p 5, Oak Ridge National Laboratory (1957)
5. A. P. Jain, Nucl. Phys., 50, p 157 (1964)
6. J. M. Otter, Nucl. Sci. Eng., 28, p 144 (1967)
7. J. M. Otter, "UNICORN - A Program to Calculate Point Cross Sections From Resonance Parameters," NAA-SR-11980, VI, Atomics International (1966)
8. W. W. Havens, Phys. Rev., 71, p 165 (1947)
9. J. E. Evans, Phys. Rev., 97, p 565 (1955)
10. R. E. Schmunk, P. D. Randolph, and R. M. Brugger, Nucl. Sci. Eng., 7, p 193 (1960)
11. M. Adib, M. Abu El-Ela, M. Salama, A. Abdel Kawy, and I. Homouda, J. Nucl. Energy, 21, p 425 (1967)
12. D. J. Hughes and R. B. Schwartz, BNL-325, 2nd Edition (1958)
13. J. L. Cook, H. Ferguson, and A. R. de L. Musgrove, "Nuclear Level Densities in Intermediate and Heavy Nuclei," AAEC/TM392, Australian Atomic Energy Commission (1966)
14. J. M. Otter, Private Communication (1970), Computer Program URF (to be published)
15. J. M. Otter, "The TRIX-I Code, An Improved Analytic Calculation of Resonance Integrals," NAA-SR-Memo-11538, Atomics International (1965)
16. R. C. Block, G. G. Slaughter, L. W. Weston, and F. C. Vonderlage, "Neutron Radiative Capture Measurements Utilizing a Large Liquid Scintillator Detector at the ORNL Fast Chopper," Neutron Time-of-Flight Methods, Saclay Conference (J. Spaepen, Ed.), EURATOM (1961)
17. M. C. Moxon and E. R. Rae, Nuclear Instr. and Meth., 24, p 445 (1963)
18. V. A. Konks, Yu. P. Popov, and F. L. Shapiro, Soviet Physics JETP, 19, p 59 (1964)
19. M. P. Fricke, W. M. Lopez, S. J. Friesenhahn, A. D. Carlson, and D. G. Costello, "Measurements of Cross Sections for the Radiative Capture of 1-kev to 1-Mev Neutrons by Mo, Rh, Gd, Ta, W, Re, Au, and ^{238}U ," Second International Conference on Nuclear Data for Reactors, II, IAEA, Vienna (1970)

20. M. C. Moxon, "The Measurement of Average Neutron Capture Cross Sections in the Mass Region Above 100," NP-17644, Harwell (England) (1968)
21. R. L. Macklin and J. H. Gibbons, Bull. Am. Phys. Soc., 11, p 167 (1966)
22. D. Kompe, Nucl. Phys., A133, p 513 (1969)
23. J. S. Brzosko, E. Gierlik, A. Soltan Jr., and Z. Wilhelmi, Nucl. Phys., A123, p 603 (1968)
24. Rex. Booth, William P. Ball, and Malcolm H. MacGregor, Phys. Rev., 112, p 226 (1958)
25. I. Bergqvist, Arkiv Fysik, 23, p 425 (1963)
26. J. A. Miskel, K. V. Marsh, M. Lindner, and R. J. Nagle, Phys. Rev., 128, p 2717 (1962)
27. J. H. Gibbons, R. L. Macklin, P. D. Miller, and J. H. Neiler, Phys. Rev., 122, p 182 (1961)
28. R. L. Macklin, J. H. Gibbons, and T. Inada, Phys. Rev., 129, p 2695 (1963)
29. V. N. Kononov and Yu. Ya Stavisskii, Soviet Atomic Energy, 19, p 1428 (1965); Soviet Journal of Nuclear Physics, 4, p 204
30. C. K. Bockelman, R. E. Peterson, R. K. Adair, and H. H. Barshall, Phys. Rev., 76, p 277 (1949)
31. V. V. Vladimirov, I. A. Radkewich, and W. W. Sokolowsky, "A Neutron Selector With Mechanical Shutter," Proceedings of the International Conference on the Peaceful Uses of Atomic Energy, Geneva 1955, 4, P/641, p 22 (1956)
32. H. W. Newson, J. H. Gibbons, H. Marshak, R. M. Williamson, R. C. Mobley, J. R. Patterson, and P. F. Nichols, Phys. Rev., 105, p 198 (1957)
33. R. H. Tabony, K. K. Seth, E. G. Bilpuch, and H. W. Newson, Bull. Am. Phys. Soc., 7, p 23 (1962)
34. R. H. Tabony, "Optical Model Parameters From Average Total Neutron Cross Sections," Ph. D. Dissertation, Duke University (1966)
35. H. Camarda and F. Rahn, Columbia University, Private Communication (1970)
36. M. Drake, Private Communication (1970), Results of the Analysis of Resonance Integrals for the American Institute of Physics Handbook
37. C. R. Pierce, D. F. Shook, and D. Bogart, "Effective Resonance Integrals of Tantalum," NASA TND-5628, Lewis Research Center (1970)
38. D. Lister, A. B. Smith, and C. L. Dunford, "Fast Neutron Scattering From the 182, 184, and 186 Isotopes of Tungsten," Phys. Rev., 162, p 1077 (1967)
39. T. Tamura, "Computer Program Jupiter I for Coupled Channel Calculations," ORNL-4152, Oak Ridge National Laboratory (1967)
40. C. L. Dunford, "2-PLUS, A Nonspherical Optical Model for Fast Neutron Cross Sections," NAA-SR-11706, Atomics International (1966)
41. C. L. Dunford, "Optical Model Analysis of Some Recent Tungsten Cross Section Measurements," NAA-SR-11973, Atomics International (1967)

42. C. L. Dunford, "A Unified Model for Analysis of Compound Nucleus Reactions," AI-AEC-12931, Atomics International (1970)
43. J. M. Blatt and V. F. Weisskopf, Theoretical Nuclear Physics, John Wiley and Sons, New York, p 627 (1952)
44. J. H. E. Mattauch, W. Thiele, and A. H. Wapstra, "1964 Atomic Mass Table," Nucl. Phys., 67, p 1 (1965)
45. P. A. Moldauer, Phys. Rev., 135, p 642 (1964)
46. P. A. Moldauer, Rev. Mod. Phys., 36, p 1074 (1964)
47. S. A. Cox, Phys. Rev., 113B, p 378 (1964)
48. V. Benzi and G. Reffo, "Fast Neutron Radiative Capture Cross-Sections of Stable Nuclei With $32 \leq Z \leq 66$," CCDN-NW10, ENEA Neutron Data Compilation Center (1969)
49. J. L. Perkin, L. P. O'Connor, and R. F. Coleman, Proc. Phys. Soc. (London), 72, p 505 (1958)
50. A. B. Smith, P. T. Guenther, and J. F. Whalen, Phys. Rev., 168, p 1344 (1968)
51. A. B. Smith, P. T. Guenther, R. Hayes, and J. F. Whalen, "Fast Neutron Scattering From Tantalum, Rhenium, and Platinum," ANL-7363, Argonne National Laboratory (1967)
52. M. Divadeenam, Dissertation Abstract, 28, p 3834B (1968) and Private Communication, Duke University (1970)
53. R. C. Martin, Bull. Am. Phys. Soc., 12, p 106 (1967)
54. R. C. Martin, "Mev Neutron Total Cross Sections of Tantalum and Tungsten Isotopes," Ph. D. Dissertation, RPI (1967)
55. B. Holmqvist and T. Wiedling, "Neutron Elastic Scattering Cross Sections—Experimental Data and Optical Model Cross Section Calculations," AE-366, Studsvik, Nyköping, Sweden (1969)
56. D. W. Miller, R. K. Adair, C. K. Bockelman, and S. E. Darden, Phys. Rev., 88, p 83 (1952)
57. Norris Nereson and Sperry Darden, Phys. Rev., 94, p 1678 (1954)
58. D. Graham Foster, Jr. and Dale W. Glasgow, Phys. Rev., C3, p 576 (1971)
59. A. Bratenahl, J. M. Peterson, and J. P. Stoering, Phys. Rev., 110, p 927 (1958)
60. Jerry P. Conner, Phys. Rev., 109, p 1268 (1958)
61. R. F. Berland, "CHAD, Code to Handle Angular Data," NAA-SR-11231 (1965)
62. M. Walt and H. H. Barschall, Phys. Rev., 93, p 1062 (1954)
63. W. S. Rogers, D. I. Garber, and E. F. Schrader, Bull. Am. Phys. Soc., 6, p 61 (1961)
64. V. C. Rogers, F. M. Clikeman, and L. E. Beghian, Trans. Am. Nucl. Soc., 12, p 746 (1969)

65. R. O. Owens and J. H. Towle, Nucl. Phys., A112, p 337 (1968)
66. L. Rosen and L. Stewart, Phys. Rev., 107, p 824 (1957)
67. D. B. Thomson, Phys. Rev., 129, p 1649 (1963)
68. H. N. Brown, W. L. Bendel, F. J. Shore, and R. A. Becker, Phys. Rev., 84, p 292 (1951)
69. C. J. Gallagher, Jr., M. Jørgensen, and O. Skilbreid, Nucl. Phys., 33, p 285 (1962)
70. V. J. Ashby, H. C. Catron, L. L. Newkirk, and C. J. Taylor, Phys. Rev., 111, p 616 (1958)
71. A. Poularikas, J. Cunningham, W. McMillan, J. McMillan, and R. W. Fink, J. Inorg. Nucl. Chem., 13, p 196 (1960)
72. W. B. Henderson, P. A. DeCorrevant, J. W. Zwick, "Evaluation and Compilation of Ta-181, W-182, W-183, W-184, and W-186 Cross Section Data for the ENDF/B File," GEMP-448, General Electric Company (1966)
73. S. Pearlstein, Nucl. Sci. Eng., 23, p 238 (1965)
74. A. Rubbino and D. Zubke, Nucl. Phys., 85, p 606 (1966)
75. K. Tsukada, S. Tanaka, M. Maruyama, and Y. Tomita, Nucl. Phys., 78, p 369 (1966)
76. S. G. Buccino, C. E. Hollandsworth, H. W. Lewis, and P. R. Bevington, Nucl. Phys., 60, p 17 (1964)
77. J. M. Blatt and V. F. Weisskopf, op cit., p 372



Atomsics International
North American Rockwell

P.O. Box 309
Canoga Park, California 91304